Am J Cancer Res 2026;16(8):3678-3693
www.ajcr.us /ISSN:2156-6976/ajcr0173760

Original Article

IL-23 promotes PD-L1 expression and tumor immune evasion via METTL16 pathway

Xueshan Pan[1,2*], Yue Wang[1*], Jingjing Luo[1,3], Xingna Dai[1], Jialin Zhang[1], Rui Zheng[1], Hui Xu[4], Yingjie Zhang[4], Jifeng Zhang[5], Zhiwei Wang[2], Tong Cao[6], Jia Ma[1,2]

[1]Bengbu Medical University Key Laboratory of Cancer Research and Clinical Laboratory Diagnosis, Bengbu Medical University, Bengbu 233030, Anhui, China; [2]Department of Biochemistry and Molecular Biology, School of Laboratory Medicine, Bengbu Medical University, Bengbu 233030, Anhui, China; [3]Department of Laboratory Medicine, Shanghai Qingpu Traditional Chinese Medicine Hospital, Shanghai 201799, China; [4]Department of Laboratory Medicine, School of Laboratory Medicine, Bengbu Medical University, Bengbu 233030, Anhui, China; [5]School of Biological Engineering and Institute of Digital Ecology and Health, Huainan Normal University, Huainan 232038, Anhui, China; [6]Department of Clinical Laboratory, The First Affiliated Hospital of Bengbu Medical University, Bengbu 233004, Anhui, China. [*]Equal contributors and co-first authors.

Received May 4, 2026; Accepted August 2, 2026; Epub August 15, 2026; Published August 30, 2026

Abstract: Interleukin-23 (IL-23) is a pivotal cytokine implicated in tumor progression and immune evasion, yet its precise molecular mechanisms remain incompletely characterized. In this study, we elucidate that IL-23 upregulates METTL16, which in turn enhances PD-L1 expression and facilitates tumor immune escape. Integrated analysis of TCGA and GEO datasets revealed the co-upregulation of IL-23 and METTL16 in lung and colon carcinomas, both of which are correlated with poor clinical outcomes. Mechanistically, IL-23 induces METTL16 expression in cancer cells via JAK-STAT3 pathway-mediated transcriptional activation. Notably, METTL16 augments PD-L1 levels via an m6A-independent mechanism by directly binding to PD-L1 and impeding its SPOP-mediated ubiquitination and proteasomal degradation. In vivo, METTL16 promotes colon cancer xenograft growth while concurrently suppressing $CD8^+$ T cell infiltration and IFN-γ secretion within the tumor microenvironment. Collectively, these findings establish the IL-23/METTL16/PD-L1 axis as a novel regulatory pathway and potential therapeutic target in cancer immunotherapy.

Keywords: IL-23, METTL16, PD-L1, colon cancer, immune evasion

Introduction

Tumor cells evade host immune surveillance primarily through the PD-1/PD-L1 axis, which suppresses T cell activity within the tumor microenvironment (TME) [1, 2]. Although immune checkpoint inhibitors targeting PD-1/PD-L1 have significantly enhanced T cell-mediated antitumor responses, their clinical benefits remain limited to a subset of patients, largely due to primary and acquired resistance [3]. Given the multifaceted regulation of PD-L1 expression, uncovering its upstream modulators is critical for overcoming resistance and improving the efficacy of cancer immunotherapy.

Interleukin-23 (IL-23) is a heterodimeric cytokine composed of p40 and p19 subunits [4], predominantly secreted by antigen-presenting cells. Upon binding to its receptor IL-23R, IL-23 activates the JAK-STAT signaling cascade, predominantly engaging STAT3, which regulates the transcription of downstream target genes. This pathway promotes the proliferation and stabilization of Th17 cells, contributing to inflammatory and autoimmune processes [5]. Emerging evidence underscores IL-23 in tumor progression [6]. For example, Calcinotto et al. demonstrated that IL-23 secreted by myeloid-derived suppressor cells (MDSCs) activates the androgen receptor (AR) pathway in prostate cancer, facilitating tumor cell survival and proliferation under androgen-deprived conditions [7]. Similarly, tumor-associated macrophage (TAM)-derived IL-23 has been shown to facilitate immune evasion in glutamine-addicted

https://doi.org/10.62347/DDRA7133

clear cell renal cell carcinoma (ccRCC) [8]. Nevertheless, the role of IL-23 in cancer remains controversial, with studies suggesting both tumor-promoting effects, such as enhancing cell survival, proliferation, and immune suppression, and tumor-suppressive functions, particularly when IL-23 is derived from tumor cells themselves [9-13]. These conflicting findings underscore the need to clarify the molecular context in which IL-23 exerts its immunomodulatory effects, particularly in relation to PD-L1 regulation and tumor immune escape.

N6-methyladenosine (m6A) is the most prevalent internal RNA modification in eukaryotes, representing a crucial epigenetic mechanism that modulates RNA metabolism. This modification is dynamically regulated by methyltransferases (writers) and demethylases (erasers), while its downstream functions are executed through specific RNA-binding proteins (readers) [14]. Among recently identified m6A writers, METTL16 has emerged as a multifunctional regulator involved in pre-mRNA splicing, mRNA stability, and translational control in mammalian cells [15-18]. Accumulating evidence reveals the context-dependent roles of METTL16 in tumorigenesis. For instance, in acute myeloid leukemia (AML), METTL16 promotes leukemogenesis by reprogramming branched-chain amino acid (BCAA) metabolism via m6A-dependent mechanisms [19]. In cholangiocarcinoma, METTL16 facilitates tumor progression via PRDM15-mediated upregulation of FGFR4 [20]. Furthermore, lactylation-modified METTL16 has been shown to induce cuproptosis in gastric cancer by mediating m6A-dependent modification of FDX1 mRNA [21]. METTL16 also maintains intracellular S-adenosylmethionine (SAM) homeostasis and redox balance, consequently suppressing lytic replication of Kaposi's sarcoma-associated herpesvirus (KSHV) and modulating KSHV-associated tumorigenesis [22]. More broadly, m6A modification serves as a master regulator of both tumor progression and anti-tumor immunity. Notably, multiple m6A regulators such as METTL3, FTO, and IGF2BP2, have been validated as promising therapeutic targets for enhancing immunotherapy efficacy [23]. Nevertheless, the specific involvement of METTL16 in tumor immune evasion awaits systematic elucidation. Recent studies have begun to explore the regulatory relationship between METTL16 and PD-L1. Wang et al. reported that METTL16 negatively regulates PD-L1 expression in colorectal cancer through an m6A-dependent mechanism by reducing PD-L1 mRNA stability, thereby enhancing antitumor immune responses [24]. Additionally, Lu et al. observed that METTL16 overexpression decreased PD-L1 expression in pancreatic ductal adenocarcinoma and is positively associated with $CD8^+$ T-cell infiltration [25]. These findings suggest that, under basal conditions, METTL16 may promote antitumor immunity through m6A-dependent epitranscriptomic regulation. Whether inflammatory signaling, such as IL-23 stimulation, induces a functional switch in METTL16 and alters its role in tumor immune evasion remains unclear.

Our research group has long been dedicated to studying the intersection of epitranscriptomic regulation and tumor immunity. In our preliminary work, through analysis of TCGA data and immune-related gene set enrichment, we observed that METTL16 expression is aberrant in multiple cancer types and significantly correlates with immune cell infiltration and immune-related pathways, suggesting its potential involvement in tumor immune regulation. However, unlike the well-studied METTL3 and METTL14, the precise role and regulatory mechanisms of METTL16 in tumor immunity remain largely unexplored. Meanwhile, IL-23, a key pro-inflammatory cytokine, plays a critical role in tumor immune evasion and represents another long-standing research interest of our group. Notably, the crosstalk between IL-23 signaling and epitranscriptomic regulation has not yet been reported. Based on the above background, we propose the following hypothesis: IL-23 activates the STAT3 signaling pathway to upregulate METTL16 expression, which in turn stabilizes PD-L1 protein through a post-translational mechanism, thereby promoting tumor immune evasion.

Based on this hypothesis, we investigate the molecular mechanism by which IL-23 upregulates METTL16 to enhance PD-L1 expression and facilitate immune escape. While IL-23 has been implicated in immunosuppressive processes within the TME, the role of METTL16 as a mediator of this pathway remain undefined. Through a combination of bioinformatic analysis and experimental validation, we delineate how IL-23 mediated METTL16 expression and

subsequently impacted on PD-L1 expression. Our findings not only elucidate a previously unrecognized IL-23/METTL16/PD-L1 axis but also highlight potential targets for improving cancer immunotherapy.

Materials and methods

Cell culture, cell transfection and infection

Human lung cancer cell lines (A549 and H1299), colorectal cancer cell lines (HCT-116, RKO, and HT-29), esophageal cancer cell line (KYSE-150), renal cancer cell line (786-0), and breast cancer cell line (MDA-MB-231) were obtained from the Cell Bank of the Chinese Academy of Sciences (Shanghai, China). All cell lines were authenticated using short tandem repeat (STR) profiling and tested for mycoplasma contamination. Cells were cultured in DMEM or RPMI-1640 medium (Gibco), supplemented with 10% fetal bovine serum (FBS; Gibco) and 1% penicillin-streptomycin (Gibco) at 37°C in a humidified incubator with 5% CO_2. Transfections with plasmids or siRNAs were performed using Lipofectamine 3000 (Invitrogen) according to the manufacturer's protocol.

Plasmids, siRNA and sgRNA

Plasmids, including METTL16 overexpression plasmid, IL-23 plasmid, STAT3 plasmid, and their respective empty vectors were constructed by Youbio Biological Technology (Hunan, China). The SPOP overexpression plasmid was constructed by Bio-research Innovation Center (Suzhou, China). All constructs were cloned into pcDNA 3.1 vector carrying with different tags (Flag, HA, His). The siRNAs targeting IL-23, METTL16 and STAT3 were purchased from Hanbio Biotechnology Co. LTD (Shanghai, China). IL-23 siRNA sequences were used as follows: siIL-23, sense: 5'-CAG CAG CUU UCA CAG AAG CUC UGC-3', antisense: 5'-GCA GAG CUU CUG UGA AAG CUG CUG-3'. METTL16 siRNA sequences were used as follows: siMETTL16-1, sense: 5'-GAA AUA GAU ACA AGG ACA ATT-3', antisense: 5'-UUG UCC UUG UAU CUA UUU CTT-3'; siMETTL16-2, sense: 5'-GGA UGC UCU UAA AGA AGA ATT-3', antisense: 5'-UUC UUC UUU AAG AGC AUC CTT-3'; siMETTL16-3, sense: 5'-GGU GAA UUA GAG UUU GUU ATT-3', antisense: 5'-UAA CAA ACU CUA AUU CAC CTT-3'. STAT3 siRNA sequences were used as follows: siSTAT3-1, sense: 5'-ACA UCC AAA UAG AAG AUA GGA CU-3', antisense: 5'-AGU CCU AUC UUC UAU UUG GAU GU-3'; siSTAT3-2, sense: 5'-CCC GUC AAC AAA UUA AGA AAC UG-3', antisense: 5'-CAG UUU CUU AAU UUG UUG ACG GG-3'.

Antibodies

Anti-IL-23 antibody (#TA372494; 1:1000) was purchased from Origene, and Anti-IL-23R antibody (#27163-1-AP; 1:1000) was purchased from Proteintech. Anti-STAT3 antibody (#sc8019; 1:1000), and anti-pSTAT3 antibody (#sc8059; 1:1000) was purchased from Santa cruz, anti-actin antibody (GB11001-100; 1:2,000) antibodies was obtained from Servicebio. Anti-METTL16 antibody (19924-1-AP; 1:2,000), Anti-Flag tag (20543-1-AP; 1:20,000), anti-PD-L1 antibody (66248-1-Ig; 1:2,000), anti-HA tag (51064-2-AP; 1:5,000) and anti-His tag (66005-1-Ig; 1:3,000) antibodies were all bought from Proteintech. Peroxidase-conjugated anti-mouse secondary antibody (70-GAM007; 1:5000) and peroxidase-conjugated anti-rabbit secondary antibody (70-GAR0072; 1:5,000) were purchased from MultiSciences Company.

RNA extraction and qPCR

Total RNA was extracted using TRIzol reagent (Invitrogen) and reverse transcribed into cDNA using PrimeScript™ RT reagent Kit (TaKaRa). Quantitative real-time PCR (qPCR) was performed using SYBR Green PCR Master Mix (TaKaRa) on a LightCycler 480 Instrument (Roche). The qPCR reaction was performed in a total volume of 20 μL containing 2 μL of cDNA template, 0.4 μL each of forward and reverse primers (10 μM), 10 μL of 2× SYBR Green Master Mix, and nuclease-free water. The thermal cycling conditions consisted of an initial denaturation at 95°C for 30 s, followed by 40 cycles of denaturation at 95°C for 10 s and combined annealing and extension at 60°C for 30 s. Relative target gene expression was calculated using the $2^{-\Delta\Delta Ct}$ method. Primers were described as follows: METTL16, Forward: 5'-TCT GAA TGG AAG AGT GAG CCT T-3', Reverse: 5'-GAG TCT CAA GGG AAC TGT GGG-3'; PD-L1, Forward: 5'-CAT TTG CTG AAC GCC CCA TA-3', Reverse: 5'-TGT CCA GAT GAC TTC GGC CT-3'; GAPDH, Forward: 5'-CAG CCT CAA GAT

CAG CA-3', Reverse: 5'-TGT GGT CAT GAG TCC TTC CA-3'.

Western blotting

Cells were collected and lysed in cold RIPA buffer supplemented with protease inhibitor cocktail (Thermo Fisher Scientific). Lysates were centrifuged at 12,000 g for 20 min at 4°C and then the liquid supernatants were collected. Protein concentrations were determined using a BCA kit (P0012, Beyotime Biotechnology). Then, proteins were separated by SDS-PAGE and transferred to PVDF membranes. Membranes were blocked with 5% skim milk and incubated with primary antibodies overnight at 4°C: anti-METTL16 (1:2000, 19924-1-AP, Proteintech), anti-IL-23 (1:1000, Origene), anti-PD-L1 (1:2000, 66248-1-Ig, Proteintech), anti-STAT3 (1:1000, Santa Cruz Biotechnology), anti-p-STAT3 (1:1000, Santa Cruz Biotechnology), and anti-Actin (1:2000, GB11001-100, Servicebio). After overnight incubation, the membranes were washed and incubated for 1 h at room temperature with horseradish peroxidase (HRP)-conjugated secondary antibodies: goat anti-mouse IgG (1:5,000; GAM007, Lianke Biotech) or goat anti-rabbit IgG (1:5,000; GAR0072, Lianke Biotech). Protein bands were detected using enhanced chemiluminescence reagents (Thermo Fisher Scientific) and imaged with a chemiluminescence detection system (Thermo Fisher Scientific) [26].

Immunoprecipitation (IP)

For immunoprecipitation experiments, cells were first lysed using a cold NP40 lysis buffer containing a protease inhibitor cocktail (Thermo Fisher Scientific). The resulting protein lysate was then incubated with magnetic beads conjugated to HA or Flag tags (Sino Biological, China). Following three washes with TBST buffer to remove non-specific binding, the proteins were eluted from the beads by heating in SDS loading buffer. The eluted samples were then subjected to SDS-PAGE electrophoresis and subsequent western blot analysis.

In vivo ubiquitination assay

To assess the in vivo ubiquitination of PD-L1, cells were cotransfected with His-tagged ubiquitin and the specified plasmids. Following a 36-hour incubation post-transfection, cells were treated with MG132 (10 μM, Sigma) for 6 hours to inhibit proteasomal degradation. Subsequently, cells were harvested and lysed in NP40 buffer. The resulting lysates were incubated with magnetic beads conjugated to HA tags. After three successive washes with TBST buffer to eliminate non-specific interactions, the bound proteins were eluted by heating in SDS loading buffer. Finally, the eluted proteins were analyzed via Western blotting to detect ubiquitinated PD-L1 species.

Protein stability analysis

To determine protein stability and measure protein half-life, the cycloheximide chase assay was employed. Cells were transfected as indicated. Following a 48-hour incubation post-transfection, cells were exposed to 20 μg/ml cycloheximide (Sigma) to inhibit new protein synthesis. At specified time intervals, cells were harvested, lysed, and protein levels were assessed via Western blotting to monitor the degradation of target proteins.

ChIP assay

ChIP assays were performed using the SimpleChIP Plus Enzymatic Chromatin IP Kit (P2078, Beyotime Biotechnology) according to the manufacturer's instructions [27]. Anti-STAT3 antibody (Cell Signaling Technology) and normal IgG were used. Primers for amplifying the METTL16 promoter region: Primer 1: Forward: 5'-ATC ACT TCA ACC CCA C-3', Reverse: 5'-CCA TCT TTG GTT GGT AG-3'; Primer 2: Forward: 5'-CCC ATA CTC ACA GGG TTA GTA-3', Reverse: 5'-CTG TTA GCT CCA AAG AGC-3'.

Luciferase reporter assay

The METTL16 promoter region was cloned into the pGL3-basic vector (Promega). Cells were co-transfected with METTL16 promoter reporter plasmids and STAT3 expression plasmid or empty vector using Lipofectamine 3000. Luciferase activity was measured 48 hours post-transfection using the Dual-Luciferase Reporter Assay System (Promega) [28].

Flow cytometry

Tumor and spleen samples were treated with red blood cell lysis buffer and incubated with fluorescently labeled antibodies for 30 minutes

on ice. Antibodies used included anti-CD45 (#103106), CD3 (#100236), CD4 (#100559), CD8 (#100753), IFN-γ (#505830) and TNF-α (#506339) was purchased from BioLegend. Data were acquired using a FACSCalibur flow cytometer (BD FACSCanto) and analyzed with FlowJo software.

Animal experiments

Six- to eight-week-old Balbc and C57BL/6 mice were purchased from the Laboratory Animal Center. All animal studies were approved by the Animal Experimentation Ethical Committee of Bengbu Medical University (project license No. 2024-228). For subcutaneous xenograft models, 5×10^6 CT26 or MC38 cells were injected into the right axilla of mice. Tumor volume and weight were measured every three days. At the end of the experiments, the mice were euthanized by intraperitoneal administration of pentobarbital sodium at 50 mg/kg to induce deep anesthesia and minimize pain and distress. Death was confirmed by the absence of respiration, heartbeat, corneal reflex, muscle tone, and normal mucosal coloration. Tumor and spleen tissues were subsequently collected for flow cytometric analysis. All animal procedures were conducted in accordance with the institutional guidelines for the care and use of laboratory animals established by Bengbu Medical University.

Statistical analysis

Statistical analyses were performed using SPSS 21 and GraphPad Prism 9, with results presented as mean ± SD. For comparisons between two groups, significance was assessed using two-tailed paired or unpaired t-tests. For comparisons among multiple groups, one-way analysis of variance (ANOVA) was performed, followed by Tukey's post hoc test. For experiments involving multiple groups measured over time, such as tumor growth curves, repeated-measures ANOVA was used, followed by Bonferroni's post hoc test for multiple comparisons. A two-sided P value < 0.05 was considered statistically significant.

Results

Expression levels and clinical significance of IL-23 and METTL16 in tumor tissues

To elucidate the expression patterns and clinical relevance of IL-23 in cancer, we conducted a systematic analysis across multiple tumor types. Initial screening using the TIMER database revealed elevated IL-23 expression in various malignancies, particularly in colon adenocarcinoma (COAD) and lung cancers (**Figure 1A**). This was further validated via the UALCAN platform, which conformed markedly higher IL-23 mRNA levels in both COAD and lung cancer specimens compared to their matched normal counterparts (**Figure 1C**, **1D**), suggesting a pan-cancer overexpression pattern predominantly in epithelial-derived tumors. Stage-stratified analysis demonstrated a progressive increase in IL23A expression from normal tissues (n = 41) through stages I to IV in COAD (**Figure 1E**). Similar stage-associated upregulation trends were observed in lung adenocarcinoma (LUAD) and lung squamous cell carcinoma (LUSC) cohorts (Figure S1B). These findings position IL23A as a potential biomarker for tumor progression in COAD, LUAD, and LUSC.

Further analysis of the TCGA-COAD dataset (41 normal vs. 471 tumor samples) reinforced IL-23 overexpression in tumor tissues (**Figure 1B**). This finding was corroborated by data from the GSE76987 dataset, which showed significantly higher IL-23A levels in malignant tissues compared to normal or precancerous samples (**Figure 1H**). Immune infiltration analysis revealed positive correlations between IL23A expression and multiple immune cell subsets in both COAD and LUAD, including B cells, $CD8^+$ T cells, $CD4^+$ T cells, macrophages, neutrophils, and dendritic cells (Figure S1A), implicating a potential role of IL-23 in shaping the tumor immune microenvironment. Clinically, Kaplan-Meier analysis showed that high IL-23A expression was significantly associated with reduced overall survival in LUAD (**Figure 1F**), underscoring its prognostic relevance and potential involvement in tumor aggressiveness.

METTL16 has been a long-standing research focus of our laboratory, and our previous studies have generated substantial preliminary evidence showing that METTL16 is aberrantly expressed across multiple tumor types and closely associated with the tumor immune microenvironment [29, 30]. To explore the epigenetic landscape associated with IL-23 signaling, we next characterized the expression profile of METTL16. Analysis of TCGA-COAD data

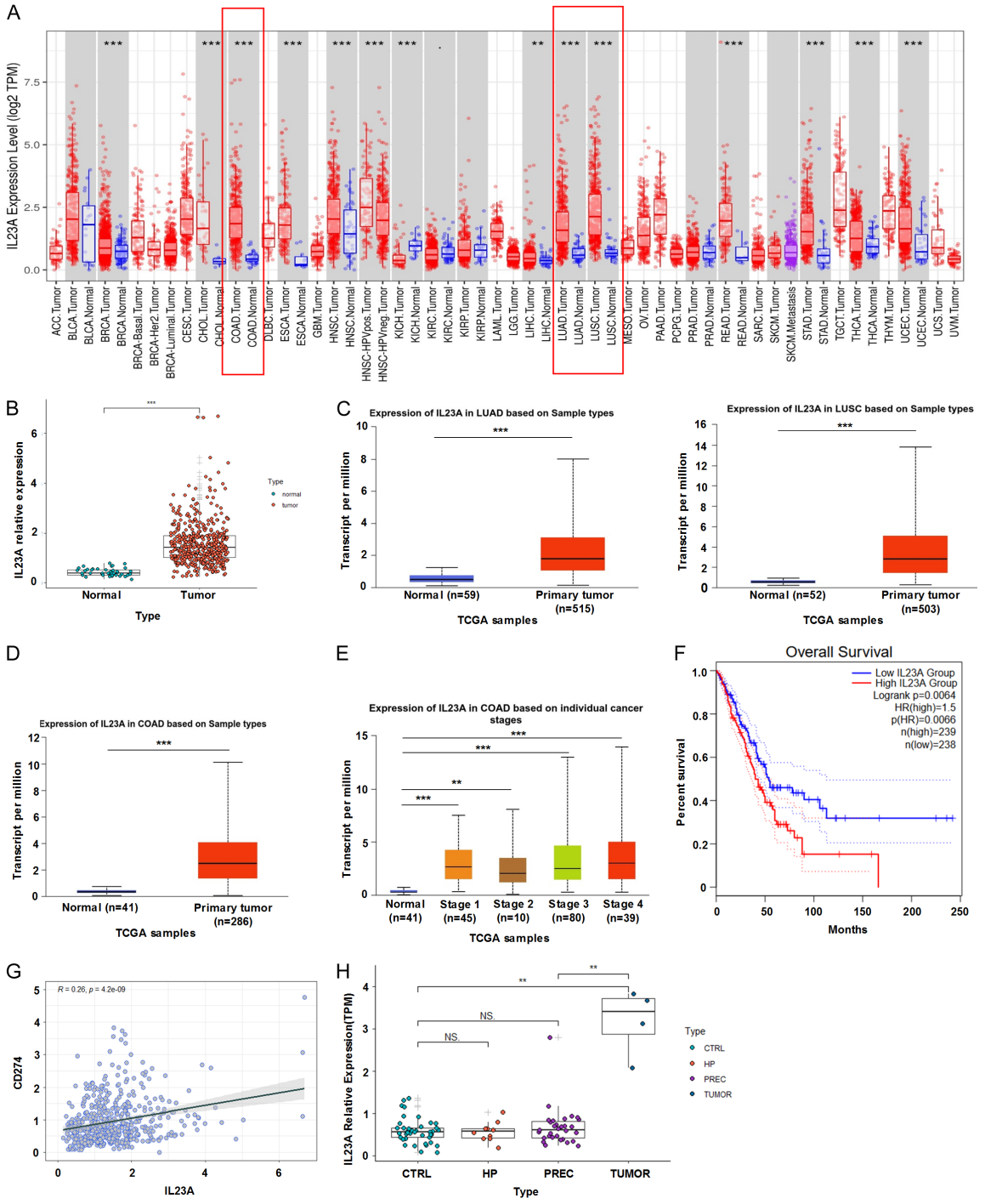

Figure 1. Expression levels and clinical significance of IL-23 in tumor tissues. A. Box plot analysis of IL23A expression across various cancer types using the TIMER database. Significantly elevated IL23A expression is observed in tumor tissues compared to normal controls. Colorectal cancer (COAD) and lung cancers (LUAD, LUSC) are highlighted in red boxes. B. Correlation analysis between IL23A expression and tumor purity in COAD, showing a significant positive correlation ($P < 0.0001$). C. Box plots comparing IL23A expression in LUAD and LUSC tumor tissues versus normal tissues. IL23A expression is significantly higher in tumors ($P < 0.0001$). D. IL23A expression in COAD stratified by tissue type (normal, primary tumor, and metastatic tumor), showing significant upregulation in tumors ($P < 0.0001$). E. Stage-specific expression of IL23A in COAD, revealing progressive upregulation with advancing clinical stage ($P < 0.0001$). F. Kaplan-Meier overall survival analysis of COAD patients stratified by IL23A expression levels. High IL23A expression correlates with reduced overall survival (log-rank $P = 0.0046$). G. Scatter plot showing a positive correlation between IL23A and METTL16 expression (R = 0.20, $P = 4.2e-06$). H. Box plot analysis of IL23A expression in normal, hyperplastic, precancerous, and tumor tissues, showing significantly elevated levels in tumor samples ($P < 0.0001$).

indicated METTL16 overexpression in colorectal tumor tissues (Figure S2A). Immune profiling using the TIME2 database demonstrated that METTL16 expression positively correlated with immune cell infiltration, including B cells, $CD8^+$ T cells, $CD4^+$ T cells, macrophages, neutrophils, and dendritic cells (Figure S2B). UALCAN analysis revealed a stage-dependent increase in METTL16 mRNA expression from stage I to IV (Figure S2C, S2D). The GSE76987 dataset also showed increased METTL16 expression in malignant versus precancerous/normal colon tissues (Figure S2G). Clinically, high METTL16 expression correlated with unfavorable overall survival in COAD patients (Figure S2E). Previous studies in pancreatic ductal adenocarcinoma have also linked high METTL16 expression to increased $CD8^+$ T-cell infiltration and immune checkpoint expression, including PD-L1, supporting a potential role for METTL16 in tumor immune regulation [25, 31]. Consistent with these findings, the positive correlation between METTL16 and CD274 (Figure S2F) provided a strong rationale for further investigation. Notably, co-expression analysis showed a strong positive correlation between IL-23A and CD274 (encoding PD-L1) across tumor samples (**Figure 1G**), implicating both IL-23 and METTL16 in the modulation of immune checkpoint pathways and tumor immune evasion.

IL-23 regulates METTL16 expression via STAT3-dependent transcriptional activation

To elucidate the mechanism by which IL-23 regulates METTL16 expression, we performed a series of in vitro experiments across multiple tumor cell lines. IL-23 knockdown significantly decreased METTL16 mRNA levels in A549 and H1299 cells compared to negative controls (NC) groups (**Figure 2A**). Conversely, recombinant human IL-23 (rhIL-23) treatment induced a dose-dependent upregulation of METTL16 mRNA in both cell lines (**Figure 2B**). Consistently, Western blot analyses conformed that rhIL-23 elevated METTL16 protein levels, whereas IL-23 silencing reduced its expression (**Figure 2C**, **2D**), indicating a positive regulatory role of IL-23 in METTL16 induction. These findings were further validated in additional cancer cell lines (Figure S3A, S3B).

Given the well-established role of STAT3 as a downstream effector in IL-23 signaling [32, 33], we next examined its involvement in METTL16 regulation. As shown in **Figure 2C**, **2D**, rhIL-23 stimulation increased p-STAT3 levels in a dose-dependent manner, while IL-23 knockdown diminished p-STAT3 expression, paralleling changes in METTL16 expression. Notably, PD-L1 protein levels also increased upon rhIL-23 stimulation in a dose-dependent fashion, consistent with the upregulation of METTL16. Additionally, IL-23R protein expression was similarly upregulated following rhIL-23 treatment, suggesting a potential positive feedback mechanism that may amplify IL-23 signaling. Overexpression of STAT3 led to a marked increase in METTL16 mRNA (**Figure 2E**) and protein levels (**Figures 2G**, S3C), while STAT3 knockdown produced the opposite effects (**Figures 2F**, **2H**, S3D). Immunofluorescence staining confirmed nuclear co-localization of STAT3-METTL16 (Figure S3E). To further confirm direct transcriptional regulation, luciferase reporter assays demonstrated that STAT3 overexpression significantly enhanced METTL16 promoter activity (**Figure 2I**). ChIP-qPCR revealed a strong enrichment of STAT3 at the METTL16 promoter region (Primer 1), in contrast to IgG controls (**Figure 2J-L**). Collectively, these results establish STAT3 as a transcriptional activator of METTL16 in response to IL-23 signaling, and further reveal that IL-23 simultaneously upregulates PD-L1 and IL-23R expression, potentially through both METTL16-dependent and -independent pathways.

METTL16 regulates PD-L1 expression in tumor cells

We next investigated whether METTL16 influences PD-L1 expression. Western blot analyses demonstrated that METTL16 overexpression significantly elevated PD-L1 protein levels in both lung and colon cancer cell lines, whereas METTL16 knockdown led to a notable reduction in PD-L1 expression (**Figure 3A**, **3B**, **3D**, **3E**). This regulatory relationship was confirmed in additional cancer cell lines (**Figure 3C**), supporting METTL16 as a positive regulator of PD-L1. Flow cytometric analysis further corroborated these findings, revealing elevated surface PD-L1 levels in METTL16-overexpressing cells across diverse cancer types, including esophageal (KYSE-150), and breast (MDA-MB-231) cancer cell lines (**Figure 3F**, **3G**).

These findings collectively indicate that METTL16 governs PD-L1 expression across multi-

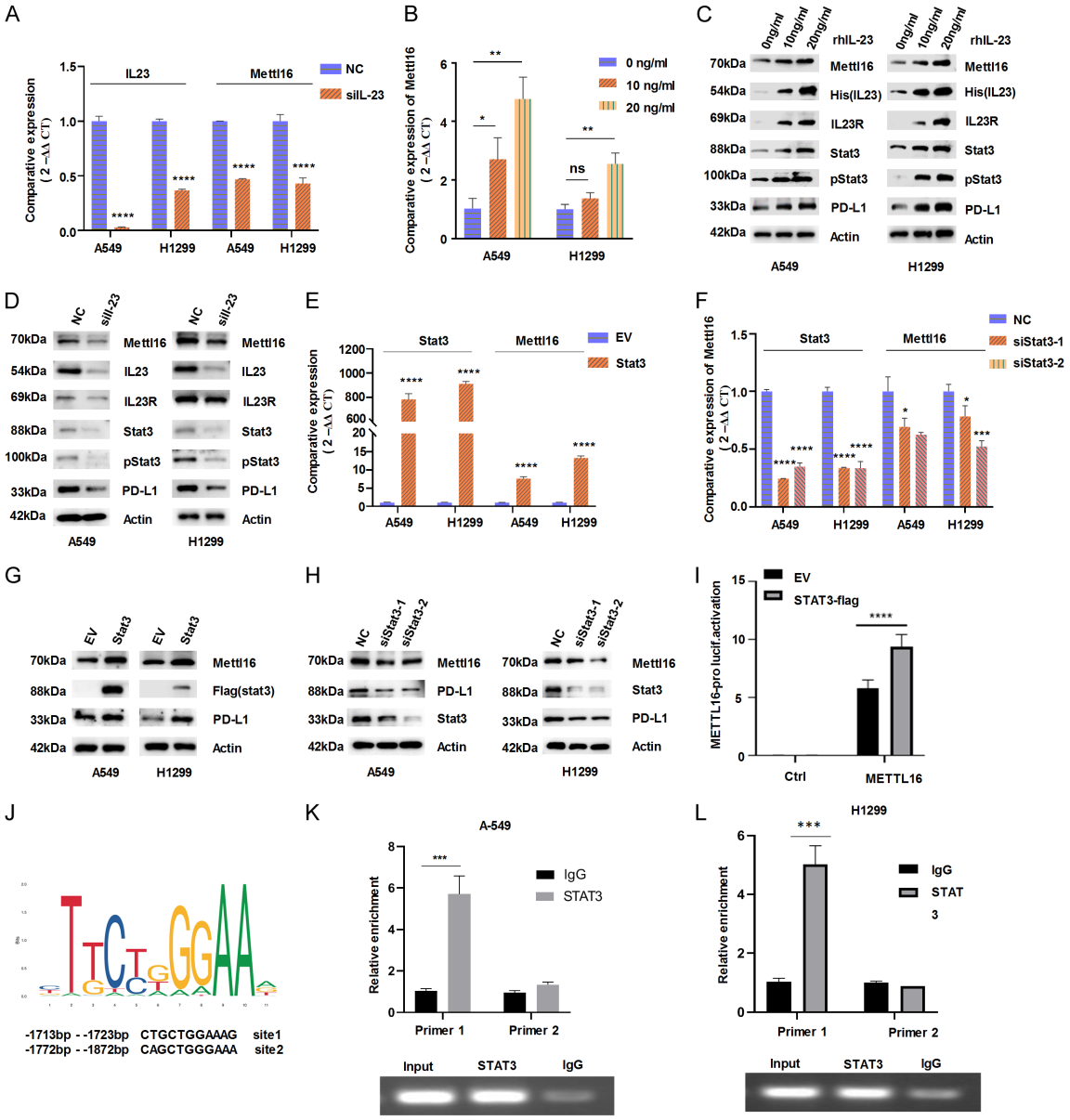

Figure 2. IL-23 upregulates METTL16 expression via the JAK-STAT3 signaling pathway. A. qRT-PCR analysis of IL-23 and METTL16 mRNA levels in A549 and H1299 cells transfected with siIL-23 or negative control (NC). Data are presented as mean ± SD (n = 3). ****P < 0.0001. B. Dose-dependent induction of METTL16 mRNA expression by rhIL-23 (0, 10, or 20 ng/mL for 24 h) in A549 and H1299 cells. P < 0.05, P < 0.01, ns: not significant. C. Western blot analysis of METTL16, IL-23, IL-23R, STAT3, phospho-STAT3, and PD-L1 in A549 and H1299 cells transfected with siIL-23 or NC. Actin serves as a loading control. D. Western blot of METTL16 and PD-L1 in A549 and H1299 cells following IL-23 knockdown. E. qRT-PCR showing METTL16 expression in A549 and H1299 cells treated with rhIL-23 (0, 10, or 20 ng/mL for 24 h). ****P < 0.0001. F. qRT-PCR of METTL16 expression in A549 and H1299 cells transfected with empty vector (EV), STAT3-flag, or siSTAT3. ****P < 0.0001. G. Western blot analysis of METTL16 and PD-L1 in A549 and H1299 cells overexpressing STAT3-flag. H. Western blot showing METTL16, Flag-STAT3, and PD-L1 expression in A549 and H1299 cells transfected with siSTAT3-1, siSTAT3-2, or NC. I. Luciferase reporter assay of METTL16 promoter activity in A549 and H1299 cells co-transfected with STAT3-flag or EV. ****P < 0.0001. J. Schematic representation of the METTL16 promoter with predicted STAT3 binding sites. K, L. ChIP-qPCR analysis of STAT3 binding to the METTL16 promoter in A549 and H1299 cells. Data are shown as mean ± SD (n = 3). ****P < 0.0001.

ple tumor types. The observed reduction of PD-L1 following IL-23 silencing (siIL-23) and its induction by rhIL-23 (**Figures 2C**, **2D**, S3A, S3B), coupled with bioinformatic co-expression anal-

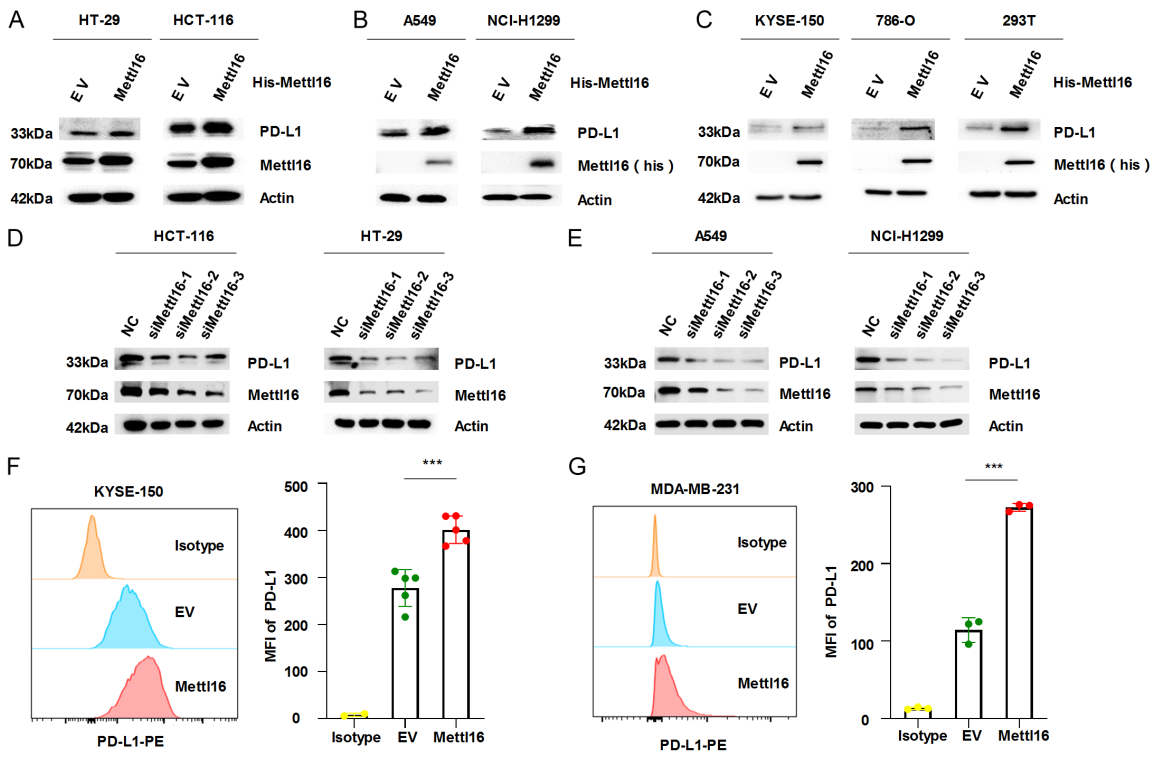

Figure 3. METTL16 regulates PD-L1 expression in tumor cells. (A) Western blot analysis of PD-L1 expression in HT-29 and HCT-116 colorectal cancer cells transfected with empty vector (EV) or METTL16 overexpression plasmid. (B) PD-L1 expression in A549 and H1299 lung cancer cells transfected with EV or METTL16 plasmid, as detected by Western blot. (C) PD-L1 protein levels in KYSE-150 (esophageal), 786-O (renal), and 293T cells following METTL16 overexpression. (D) PD-L1 expression in HT-29 and HCT-116 cells transfected with METTL16 siRNA or negative control (NC). (E) Western blot analysis of PD-L1 in A549 and H1299 cells following METTL16 knockdown. (F, G) Increased membrane PD-L1 levels were observed upon METTL16 overexpression in KYSE-150 (F) and MDA-MB-231 cells (G).

yses of IL-23 and PD-L1 (**Figure 1G**), position METTL16 as a key mechanistic link between IL-23 signaling and PD-L1 upregulation. Thus, our data define the IL-23-METTL16-PD-L1 axis as a crucial pathway mediating tumor immune evasion and a potential target for immunotherapeutic intervention.

METTL16 inhibits SPOP-mediated ubiquitination and degradation of PD-L1

To elucidate the molecular mechanism by which METTL16 regulates PD-L1 expression, we first examined public m6A-seq datasets (GSE90914, GSE182607) to determine whether METTL16 modulates PD-L1 in an m6A-dependent manner. These datasets did not support m6A modification of PD-L1 by METTL16. Consistently, qPCR analysis revealed that neither METTL16 knockdown nor overexpression significantly altered PD-L1 mRNA levels (**Figures 4A**, S4A), indicating that PD-L1 is regulated by METTL16 at a post-transcriptional level. Given that PD-L1 expression can be modulated through the ubiquitin-proteasome system, we treated METTL16-deficient cells with proteasome inhibitor MG132. This treatment rescued the METTL16 knockdown-induced reduction in PD-L1 protein levels (**Figures 4B**, S4B), implicating enhanced proteasomal degradation in the absence of METTL16. Protein stability assays further confirmed that METTL16 depletion shortened the half-life of PD-L1 (**Figures 4C**, **4D**, S4C, S4D), reinforcing the notion of post-translational regulation. Co-IP experiments verified a specific interaction between METTL16 and PD-L1 (**Figures 4E**, S4E).

Previous studies have established SPOP as a key E3 ubiquitin ligase that directly interacts with PD-L1 and promotes its K48-linked polyubiquitination and proteasomal degradation [34, 35]. Our group has also published several studies examining the functions and molecular mechanisms of SPOP in cancer development

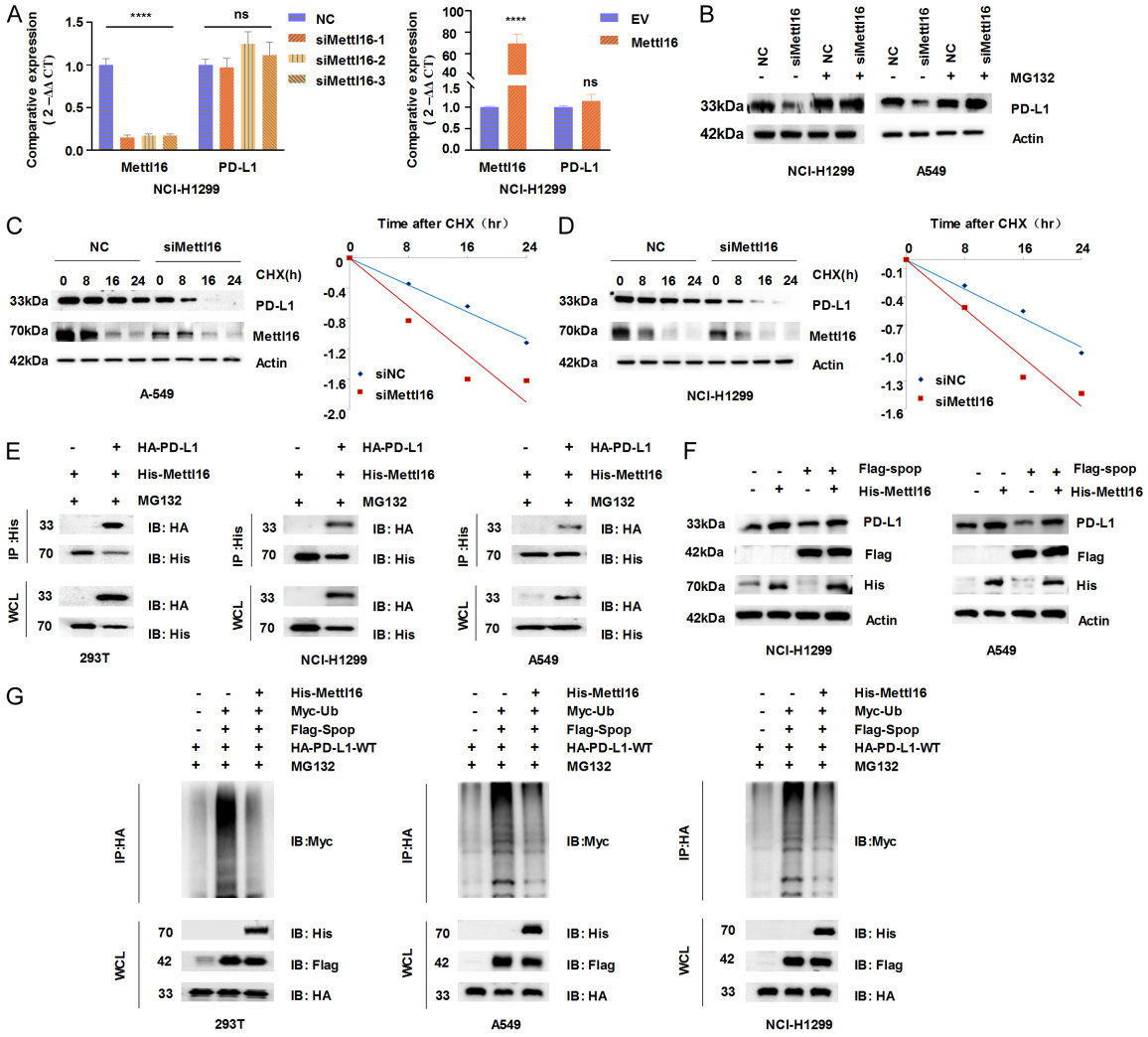

Figure 4. METTL16 inhibits SPOP-mediated PD-L1 ubiquitination and degradation. A. qRT-PCR analysis of METTL16 and PD-L1 expression in NCI-H1299 cells transfected with METTL16 siRNA or EV (left), and with METTL16 overexpression plasmid or EV (right). B. Western blot analysis of PD-L1 protein levels in NCI-H1299 and A549 cells transfected with METTL16 siRNA or NC, with or without MG132 treatment (10 μM for 6 h). MG132 restores PD-L1 levels suppressed by METTL16 knockdown. C, D. Cycloheximide (CHX) chase assays in A549 and NCI-H1299 cells transfected with METTL16 siRNA or NC. Cells were treated with CHX (20 μg/mL) for 0, 8, 16, or 24 h, followed by Western blot analysis to assess PD-L1 protein degradation. E. Co-immunoprecipitation (IP) and immunoblot (IB) analysis of PD-L1 ubiquitination in 293T, NCI-H1299, and A549 cells transfected with the indicated plasmids. Cells were pre-treated with MG132 (10 μM, 6 h) prior to harvesting. F. Western blot analysis of whole-cell lysates (WCLs) from NCI-H1299 and A549 cells transfected with control or experimental plasmids to examine PD-L1 and SPOP expression. G. Ubiquitination assay via IP and IB in 293T, A549, and NCI-H1299 cells transfected with the indicated plasmids. MG132 (10 μM) was applied for 6 h before cell collection.

and progression. This established expertise, together with prior evidence identifying SPOP as a major E3 ligase of PD-L1, provided a strong rationale for prioritizing SPOP in the present study [36-40]. Our results demonstrate that METTL16 prevents SPOP-induced downregulation of PD-L1 (**Figures 4F**, S4F). Ubiquitination assays revealed that METTL16 overexpression substantially attenuates SPOP-mediated ubiquitination of PD-L1 (**Figures 4G**, S4G). A METTL16-only control was included in 293T cells and showed no nonspecific signal (data not shown). Our data indicate that METTL16 stabilizes PD-L1 by shielding it from SPOP-dependent ubiquitination and proteasomal degradation. Collectively, these findings establish a novel mechanism by which that METTL16 stabilizes PD-L1 protein through direct binding,

thereby sterically hindering SPOP access and attenuating PD-L1 ubiquitination and subsequent degradation.

METTL16 facilitates tumor immune evasion in vivo

Previous studies reported that METTL16 downregulates PD-L1 and influences immune evasion in colorectal cancer [24, 41]. To explore the role of METTL16 in vivo function, we employed subcutaneous tumor models using CT26 and MC38 murine colon cancer cells with METTL16 knockdown or overexpression (**Figure 5A**). In the CT26 model, METTL16 knockdown significantly reduced tumor growth, as reflected by reduced tumor volume and weight compared to controls (**Figure 5B-D**). Conversely, METTL16 overexpression accelerated tumor growth (Figure S5A-C). METTL16 overexpression also led to shortened mouse survival (Figure S5D). Similar results were obtained in the MC38 model (Figure S5F-H). Crucially, METTL16 failed to promote tumor growth in immunodeficient nude mice (Figure S6A, S6B), establishing its immune-dependent oncogenic function.

Analysis of the tumor immune microenvironment revealed that METTL16 knockdown increased infiltration of immune cells, particularly $CD4^+$ and $CD8^+$ T cells (**Figure 5E**). Furthermore, $CD8^+$ T cells from METTL16-deficient tumors exhibited higher IFN-γ and TNF-α production, indicative of enhanced cytotoxic activity (**Figure 5F**). Conversely, METTL16 overexpression diminished $CD8^+$ T cell recruitment and IFN-γ secretion (Figure S5E, S5I, S5J). Splenic immune profiling showed elevated $CD8^+$ T cell proportions in METTL16-knockdown mice, without significant change in $CD4^+$ T cell populations (**Figure 5G**). Collectively, these findings demonstrate that METTL16 promotes immune evasion by limiting cytotoxic T cell infiltration and function, thereby fostering an immunosuppressive tumor microenvironment. This underscores the role of METTL16 as a key immune modulator and a potential target for reversing tumor immune escape (**Figure 6**).

Discussion

Tumor immune evasion represents a fundamental mechanism in cancer progression, allowing malignant cells to escape immune-mediated destruction and persist in the host [42]. Among the key immune checkpoint pathways, the PD-1/PD-L1 axis plays a critical role in suppressing antitumor immune responses [43]. PD-L1, expressed on tumor cells, binds to PD-1 receptors on T cells, leading to the inhibition of T-cell activation, proliferation, and cytokine production, thereby facilitating immune evasion [44, 45]. Although immune checkpoint inhibitors targeting the PD-1/PD-L1 pathway have revolutionized cancer treatment, both intrinsic and acquired resistances remain a major clinical obstacle. This underscores the critical need to elucidate the upstream regulatory mechanisms of PD-L1 expression to uncover novel therapeutic targets and enhance immunotherapy efficacy.

IL-23 is a proinflammatory cytokine that has emerged as an important modulator of tumor immunology. Upon engaging its receptor IL-23R, IL-23 activates the JAK-STAT signaling cascade, predominantly through STAT3, to modulate downstream gene expression [4]. In addition to its well-established role in autoimmune diseases such as psoriasis and Crohn's disease, IL-23 promotes Th17 cell expansion and stimulates the secretion of proinflammatory cytokines including IL-17A, IL-22, and TNF-α. Several biologics targeting IL-23 (e.g., ustekinumab, guselkumab, risankizumab) have received clinical approval for inflammatory disorders [5]. Nevertheless, the precise mechanisms by which IL-23 contributes to tumor immune evasion in cancer remain incompletely understood.

Concurrently, METTL16 has gained attention as a multifunctional m6A methyltransferase involved in RNA modification, gene expression regulation, and cellular stress responses [41]. For example, Sun et al. revealed that lactylation-modified METTL16 mediates FDX1 m6A modification to promote cuproptosis in gastric cancer [21]. Shi et al. identified that METTL16 regulates UBXN1 expression through both transcriptional and post-transcriptional mechanisms in gastric malignancies [46]. Despite these emerging roles, contribution of METTL16 to tumor immune evasion and its interplay with canonical immunosuppressive pathways, such as PD-L1 signaling, has not been fully elucidated.

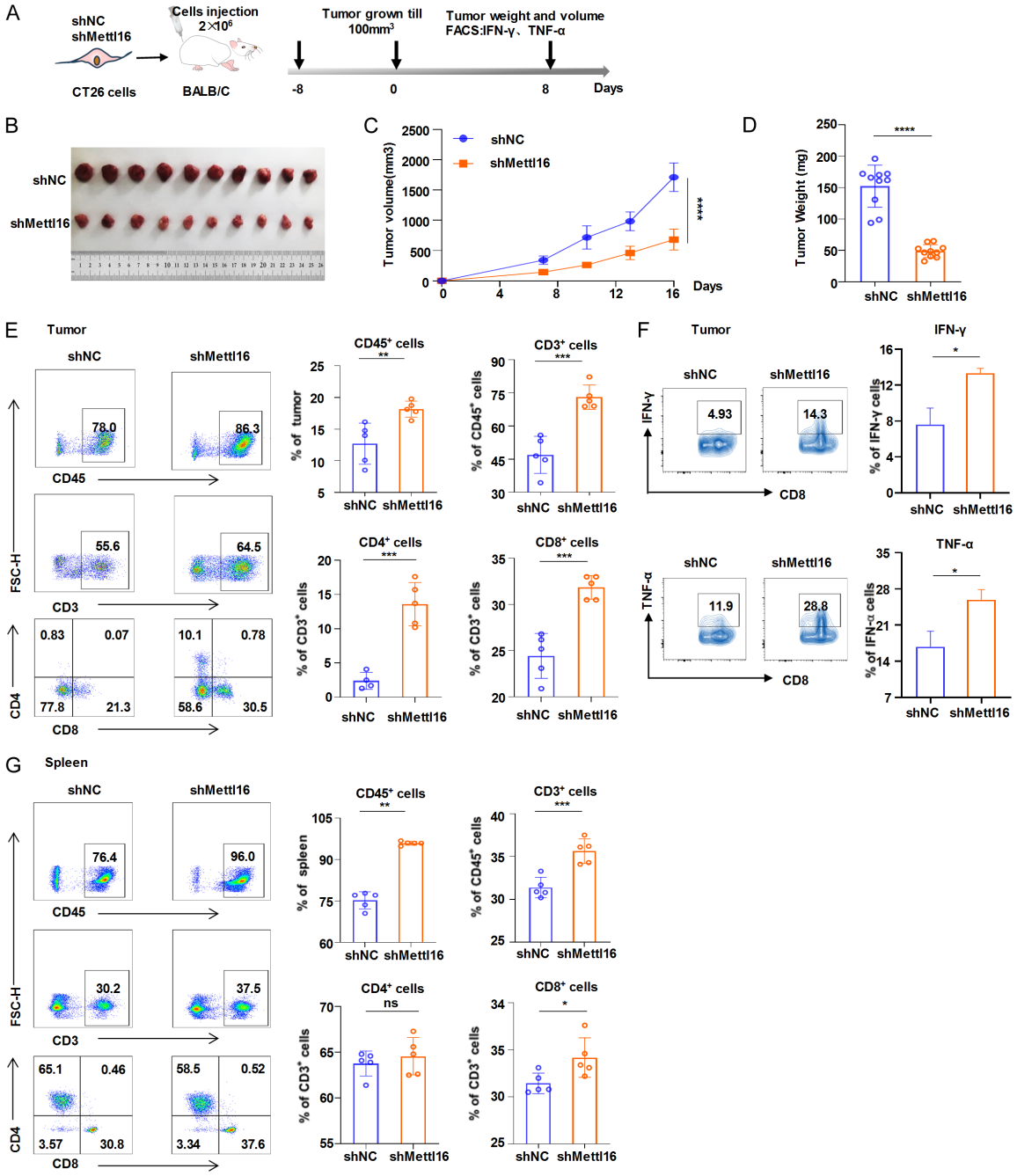

Figure 5. METTL16 promotes tumor immune evasion in vivo. (A) Schematic diagram illustrating the experimental design for colon cancer xenograft modeling in BALB/c mice using METTL16 knockdown cells. (B) Representative images of tumors excised from BALB/c mice (n = 10) subcutaneously injected with stable METTL16 knockdown or control CT26 cells. (C, D) Quantification of tumor weight (C) and tumor volume (D) in control and METTL16 knockdown groups. Data are presented as mean ± SD. ****P < 0.0001 vs. control. (E) Flow cytometry analysis of tumor-infiltrating immune cells ($CD45^+$, $CD3^+$, $CD4^+$, and $CD8^+$) in tumors from METTL16 knockdown and control mice (n = 5). **P < 0.01, ***P < 0.001. (F) Proportion of IFN-γ^+ and TNF-α^+ $CD8^+$ T cells in tumor samples, as assessed by flow cytometry. *P < 0.05 vs. control. (G) Flow cytometry analysis of splenic immune cell subsets ($CD45^+$, $CD3^+$, $CD4^+$, $CD8^+$) in METTL16 knockdown and control mice (n = 5). *P < 0.05, **P < 0.01, ***P < 0.001.

This study defines the IL-23/METTL16/PD-L1 axis as a novel regulatory pathway mediating tumor immune evasion and highlights its potential as a therapeutic target in cancer immunotherapy. Previous studies have reported critical roles of METTL16 in colon cancer. Wang et al.

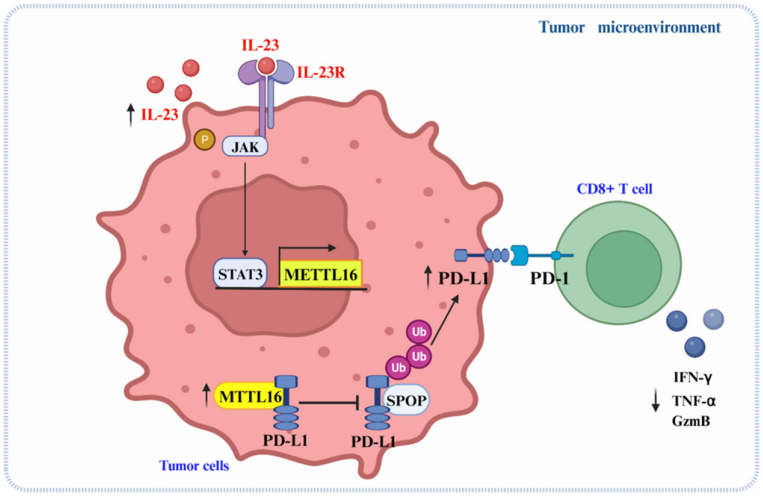

Figure 6. Schematic model depicting the IL-23/STAT3/METTL16/PD-L1 axis in tumor immune evasion. IL-23 activates STAT3 to induce METTL16, which stabilizes PD-L1 protein by blocking SPOP-mediated degradation, leading to immune escape.

demonstrated that METTL16 overexpression inhibits colon cancer cell growth and downregulates PD-L1 expression in vitro, while enhancing T cell viability and reducing apoptosis in co-culture systems, suggesting an anti-tumor immune effect [24]. Wei et al. [47] and Li et al. [48] identified METTL16 as an oncogenic factor that promotes colon cancer progression through SOGA1 upregulation via m6A-dependent mechanisms. These discrepancies underscore the context-specific functions of METTL16, likely influenced by differences in cell type, tumor microenvironment, and regulatory networks. Notably, both our study and the previous investigations by Wang et al. [24] examined the regulation of PD-L1 by METTL16, but reported opposite regulatory effects. Wang et al. showed that METTL16 negatively regulates PD-L1 through m6A modification and reduced PD-L1 mRNA stability. In contrast, our study reveals that activation of the IL-23/STAT3 signaling pathway transcriptionally upregulates METTL16, which subsequently stabilizes PD-L1 protein through an m6A-independent post-translational mechanism. Specifically, METTL16 directly interacts with PD-L1 and inhibits SPOP-mediated ubiquitination and degradation. This apparent discrepancy may reflect differences in signaling context, as previous studies were conducted largely under basal culture conditions, whereas our study specifically investigated IL-23-driven inflammatory signaling. Collectively, these findings indicate that METTL16-mediated regulation of PD-L1 is highly context dependent and may undergo a functional switch in response to microenvironmental inflammatory signals. Our in vitro and in vivo assays consistently demonstrated that METTL16 upregulates PD-L1 protein levels and promotes immune escape. METTL16 knockdown not only inhibited tumor growth but also enhanced $CD4^+$ and $CD8^+$ T cell infiltration and effector cytokine production, whereas overexpression impaired cytotoxic T cell recruitment and accelerated tumor progression. These findings clarify METTL16 as an immune evasion factor and emphasize its context-dependent function within the tumor microenvironment. Although the present study demonstrates that IL-23 upregulates METTL16 expression via the STAT3 signaling pathway and subsequently stabilizes PD-L1 protein, whether STAT3 directly binds to the METTL16 promoter remains to be fully elucidated. Bioinformatics analysis revealed several potential STAT3 binding sites within the METTL16 promoter region. Consistent with this, we observed that IL-23 treatment induced STAT3 phosphorylation and increased METTL16 expression, effects that were abrogated by a STAT3 inhibitor. Collectively, these findings suggest that STAT3 may directly regulate METTL16 transcription. However, direct evidence, such as ChIP-qPCR assays, is still needed to confirm the physical interaction between STAT3 and the METTL16 promoter. Future studies employing ChIP-qPCR will help delineate the precise binding sites and their dynamics upon IL-23 stimulation, thereby further clarifying the transcriptional regulatory mechanism of the IL-23/STAT3/METTL16 axis.

In summary, this work uncovers a previously unrecognized IL-23/STAT3/METTL16 axis that stabilizes PD-L1 and enables tumor immune escape. Targeting this pathway may offer a novel strategy to overcome resistance to PD-1/PD-L1 blockade and improve outcomes in cancer immunotherapy. Future investigations should explore whether METTL16 similar-

ly regulates other immune checkpoint proteins and how its function varies across tumor types. Additionally, given that this study was primarily based on in vitro and murine models, further validation using clinical samples is essential. Elucidating the broader role of METTL16 in tumor immunity will be critical for translating these mechanistic insights into effective, clinically actionable strategies.

Acknowledgements

ChatGPT 5.5 Thinking, developed by OpenAI, was used during manuscript preparation exclusively for language polishing, grammar correction, editorial refinement, and improvement of wording. This work was supported by grant from Natural Science Foundation of Anhui Province (2308085MH269), Anhui Provincial Department of Education Outstanding Young Teachers Development Program in Universities (YQZD2024028), Bengbu Medical University's Incubation Project under the National Natural Science Foundation of China (2024byfy003), Key Project from Natural Science Foundation of Education Department of Anhui Province (2025AHGXZK30181), and Bengbu Medical University Postgraduate Innovation Project (Byycx25021).

Disclosure of conflict of interest

None.

Address correspondence to: Zhiwei Wang and Jia Ma, Department of Biochemistry and Molecular Biology, School of Laboratory Medicine, Bengbu Medical University, Bengbu 233030, Anhui, China. E-mail: zhiweichina@126.com (ZWW); majiamj@bbmc.edu.cn (JM); Tong Cao, Department of Clinical Laboratory, The First Affiliated Hospital of Bengbu Medical University, Bengbu 233004, Anhui, China. E-mail: caotong1027@163.com

References

[1] Ren D, Hua Y, Yu B, Ye X, He Z, Li C, Wang J, Mo Y, Wei X, Chen Y, Zhou Y, Liao Q, Wang H, Xiang B, Zhou M, Li X, Li G, Li Y, Zeng Z and Xiong W. Correction to: predictive biomarkers and mechanisms underlying resistance to PD1/PD-L1 blockade cancer immunotherapy. Mol Cancer 2020; 19: 31.

[2] Yamaguchi H, Hsu JM, Yang WH and Hung MC. Mechanisms regulating PD-L1 expression in cancers and associated opportunities for novel small-molecule therapeutics. Nat Rev Clin Oncol 2022; 19: 287-305.

[3] Godiyal Y, Maheshwari D, Taniguchi H, Zinzuwadia SS, Morera-Díaz Y, Tewari D and Bishayee A. Role of PD-1/PD-L1 signaling axis in oncogenesis and its targeting by bioactive natural compounds for cancer immunotherapy. Mil Med Res 2024; 11: 82.

[4] Verstockt B, Salas A, Sands BE, Abraham C, Leibovitzh H, Neurath MF and Vande Casteele N; Alimentiv Translational Research Consortium (ATRC). IL-12 and IL-23 pathway inhibition in inflammatory bowel disease. Nat Rev Gastroenterol Hepatol 2023; 20: 433-446.

[5] Tait Wojno ED, Hunter CA and Stumhofer JS. The immunobiology of the interleukin-12 family: room for discovery. Immunity 2019; 50: 851-870.

[6] Yan J, Smyth MJ and Teng MWL. Interleukin (IL)-12 and IL-23 and their conflicting roles in cancer. Cold Spring Harb Perspect Biol 2018; 10: a028530.

[7] Calcinotto A, Spataro C, Zagato E, Di Mitri D, Gil V, Crespo M, De Bernardis G, Losa M, Mirenda M, Pasquini E, Rinaldi A, Sumanasuriya S, Lambros MB, Neeb A, Lucianò R, Bravi CA, Nava-Rodrigues D, Dolling D, Prayer-Galetti T, Ferreira A, Briganti A, Esposito A, Barry S, Yuan W, Sharp A, de Bono J and Alimonti A. IL-23 secreted by myeloid cells drives castration-resistant prostate cancer. Nature 2018; 559: 363-369.

[8] Monjaras-Avila CU, Lorenzo-Leal AC, Luque-Badillo AC, D'Costa N, Chavez-Muñoz C and Bach H. The tumor immune microenvironment in clear cell renal cell carcinoma. Int J Mol Sci 2023; 24: 7946.

[9] Punkenburg E, Vogler T, Büttner M, Amann K, Waldner M, Atreya R, Abendroth B, Mudter J, Merkel S, Gallmeier E, Rose-John S, Neurath MF and Hildner K. Batf-dependent Th17 cells critically regulate IL-23 driven colitis-associated colon cancer. Gut 2016; 65: 1139-1150.

[10] Richter C, Herrero San Juan M, Weigmann B, Bergis D, Dauber K, Muders MH, Baretton GB, Pfeilschifter JM, Bonig H, Brenner S and Radeke HH. Defective IL-23/IL-17 axis protects p47phox-/- mice from colon cancer. Front Immunol 2017; 8: 44.

[11] Shan BE, Hao JS, Li QX and Tagawa M. Antitumor activity and immune enhancement of murine interleukin-23 expressed in murine colon carcinoma cells. Cell Mol Immunol 2006; 3: 47-52.

[12] Chen L, Chen H, Ye J, Ge Y, Wang H, Dai E, Ren J, Liu W, Ma C, Ju S, Guo ZS, Liu Z and Bartlett DL. Intratumoral expression of interleukin 23 variants using oncolytic vaccinia virus elicit potent antitumor effects on multiple tumor mod-

els via tumor microenvironment modulation. Theranostics 2021; 11: 6668-6681.
[13] Hewitt SL, Bai A, Bailey D, Ichikawa K, Zielinski J, Karp R, Apte A, Arnold K, Zacharek SJ, Iliou MS, Bhatt K, Garnaas M, Musenge F, Davis A, Khatwani N, Su SV, MacLean G, Farlow SJ, Burke K and Frederick JP. Durable anticancer immunity from intratumoral administration of IL-23, IL-36γ, and OX40L mRNAs. Sci Transl Med 2019; 11: eaat9143.
[14] Zaccara S, Ries RJ and Jaffrey SR. Reading, writing and erasing mRNA methylation. Nat Rev Mol Cell Biol 2019; 20: 608-624.
[15] Pendleton KE, Chen B, Liu K, Hunter OV, Xie Y, Tu BP and Conrad NK. The U6 snRNA m(6)A methyltransferase METTL16 regulates SAM synthetase intron retention. Cell 2017; 169: 824-835, e814.
[16] Shima H, Matsumoto M, Ishigami Y, Ebina M, Muto A, Sato Y, Kumagai S, Ochiai K, Suzuki T and Igarashi K. S-adenosylmethionine synthesis is regulated by selective N(6)-adenosine methylation and mRNA degradation involving METTL16 and YTHDC1. Cell Rep 2017; 21: 3354-3363.
[17] Mendel M, Delaney K, Pandey RR, Chen KM, Wenda JM, Vågbø CB, Steiner FA, Homolka D and Pillai RS. Splice site m(6)A methylation prevents binding of U2AF35 to inhibit RNA splicing. Cell 2021; 184: 3125-3142, e3125.
[18] Su R, Dong L, Li Y, Gao M, He PC, Liu W, Wei J, Zhao Z, Gao L, Han L, Deng X, Li C, Prince E, Tan B, Qing Y, Qin X, Shen C, Xue M, Zhou K, Chen Z, Xue J, Li W, Qin H, Wu X, Sun M, Nam Y, Chen CW, Huang W, Horne D, Rosen ST, He C and Chen J. METTL16 exerts an m(6)A-independent function to facilitate translation and tumorigenesis. Nat Cell Biol 2022; 24: 205-216.
[19] Han L, Dong L, Leung K, Zhao Z, Li Y, Gao L, Chen Z, Xue J, Qing Y, Li W, Pokharel SP, Gao M, Chen M, Shen C, Tan B, Small A, Wang K, Zhang Z, Qin X, Yang L, Wunderlich M, Zhang B, Mulloy JC, Marcucci G, Chen CW, Wei M, Su R, Chen J and Deng X. METTL16 drives leukemogenesis and leukemia stem cell self-renewal by reprogramming BCAA metabolism. Cell Stem Cell 2023; 30: 52-68, e13.
[20] Liu N, Zhang J, Chen W, Ma W and Wu T. The RNA methyltransferase METTL16 enhances cholangiocarcinoma growth through PRDM15-mediated FGFR4 expression. J Exp Clin Cancer Res 2023; 42: 263.
[21] Sun L, Zhang Y, Yang B, Sun S, Zhang P, Luo Z, Feng T, Cui Z, Zhu T, Li Y, Qiu Z, Fan G and Huang C. Lactylation of METTL16 promotes cuproptosis via m(6)A-modification on FDX1 mRNA in gastric cancer. Nat Commun 2023; 14: 6523.
[22] Zhang X, Meng W, Feng J, Gao X, Qin C, Feng P, Huang Y and Gao SJ. METTL16 controls Kaposi's sarcoma-associated herpesvirus replication by regulating S-adenosylmethionine cycle. Cell Death Dis 2023; 14: 591.
[23] Li W, Hao Y, Zhang X, Xu S and Pang D. Targeting RNA N(6)-methyladenosine modification: a precise weapon in overcoming tumor immune escape. Mol Cancer 2022; 21: 176.
[24] Wang A, Sun Y, Wang X, Yan Z, Wang D, Zeng L and Lu Q. m(6)A methyltransferase METTL16 mediates immune evasion of colorectal cancer cells via epigenetically regulating PD-L1 expression. Aging (Albany NY) 2023; 15: 8444-8457.
[25] Lu L, Zheng D, Qu J, Zhuang Y, Peng J, Lan S, Zhang S and Huang F. METTL16 predicts a favorable outcome and primes antitumor immunity in pancreatic ductal adenocarcinoma. Front Cell Dev Biol 2022; 10: 759020.
[26] Cao T, Zheng R, Wang Y, Yu Z, Huang H, Chen Y, Pan X, Gao Y, Song W, Xia J, Xu H and Ma J. FBXO9 promotes anti-tumor immunity via degradation of PD-L1 in pancreatic cancer. Front Immunol 2026; 16: 1726825.
[27] Nelson JD, Denisenko O and Bomsztyk K. Protocol for the fast chromatin immunoprecipitation (ChIP) method. Nat Protoc 2006; 1: 179-85.
[28] Clément T, Salone V and Rederstorff M. Dual luciferase gene reporter assays to study miRNA function. Methods Mol Biol 2015; 1296: 187-98.
[29] Ji H, Zhang JA, Liu H, Li K, Wang ZW and Zhu X. Comprehensive characterization of tumor microenvironment and m6A RNA methylation regulators and its effects on PD-L1 and immune infiltrates in cervical cancer. Front Immunol 2022; 13: 976107.
[30] Zeng X, Wang X, Wang J, Zheng R, Zhang Y, Li T, Ma J and Pan X. METTL16 antagonizes astaxanthin-induced ferroptosis in colorectal cancer cells. Transl Cancer Res 2026; 15: 9.
[31] Yi T, Wang C, Ye X, Lin J, Lin C, Qin F, Yang W, Ye Y, Ning D, Lan J, Li H, Luo C, Ma J and Wei Z. METTL16 inhibits pancreatic cancer proliferation and metastasis by promoting MROH8 RNA stability and inhibiting CAPN2 expression - experimental studies. Int J Surg 2024; 110: 7701-7719.
[32] Liang Z, Tang Z, Zhu C, Li F, Chen S, Han X, Zheng R, Hu X, Lin R, Pei Q, Yin C, Wang J, Tang C, Cao N, Zhao J, Wang R, Li X, Luo N, Wen Q, Yu J, Li J, Xia X, Zheng X, Wang X, Huang N, Zhong Z, Mo C, Chen P, Wang Y, Fan J, Guo Y, Zhong H, Liu J, Peng Z, Mao H, Shi GP, Bonventre JV, Chen W and Zhou Y. Intestinal CXCR6(+) ILC3s migrate to the kidney and exacerbate renal fibrosis via IL-23 receptor signaling en-

hanced by PD-1 expression. Immunity 2024; 57: 1306-1323.e1308.
[33] Fan L and Zhou L. Anti-IL-23 exerted protective effects on cerebral ischemia-reperfusion injury through JAK2/STAT3 signaling pathway. Mol Biol Rep 2021; 48: 3475-3484.
[34] Zhang J, Bu X, Wang H, Zhu Y, Geng Y, Nihira NT, Tan Y, Ci Y, Wu F, Dai X, Guo J, Huang YH, Fan C, Ren S, Sun Y, Freeman GJ, Sicinski P and Wei W. Author correction: cyclin D-CDK4 kinase destabilizes PD-L1 via cullin 3-SPOP to control cancer immune surveillance. Nature 2019; 571: E10.
[35] Tian S, Xu M, Geng X, Fang J, Xu H, Xue X, Hu H, Zhang Q, Yu D, Guo M, Zhang H, Lu J, Guo C, Wang Q, Liu S and Zhang W. Network medicine-based strategy identifies maprotiline as a repurposable drug by inhibiting PD-L1 expression via targeting SPOP in cancer. Adv Sci (Weinh) 2025; 12: e2410285.
[36] Dai X, Wang Z and Wei W. SPOP-mediated degradation of BRD4 dictates cellular sensitivity to BET inhibitors. Cell Cycle 2017; 16: 2326-2329.
[37] Wang L, Lin M, Chu M, Liu Y, Ma J, He Y and Wang ZW. SPOP promotes ubiquitination and degradation of LATS1 to enhance kidney cancer progression. EBioMedicine 2020; 56: 102795.
[38] Wang Z, Song Y, Ye M, Dai X, Zhu X and Wei W. The diverse roles of SPOP in prostate cancer and kidney cancer. Nat Rev Urol 2020; 17: 339-350.
[39] Cheng J, Guo J, Wang Z, North BJ, Tao K, Dai X and Wei W. Functional analysis of Cullin 3 E3 ligases in tumorigenesis. Biochim Biophys Acta Rev Cancer 2018; 1869: 11-28.
[40] Song Y, Xu Y, Pan C, Yan L, Wang ZW and Zhu X. The emerging role of SPOP protein in tumorigenesis and cancer therapy. Mol Cancer 2020; 19: 2.
[41] Zhao Y, Gong T, Li H, Lin H, Yu M, Luo Y, Zhong M and Qin J. METTL16-mediated m6A modification of MSM01 modulates cholesterol metabolism and activates MAPK-p38/NF-κB signaling in colorectal cancer. J Exp Clin Cancer Res 2026; 45: 121.
[42] Liu QQ, Dong ZK, Wang YF and Jin WL. Reprogramming neural-tumor crosstalk: emerging therapeutic dimensions and targeting strategies. Mil Med Res 2025; 12: 73.
[43] Guo D, Tong Y, Jiang X, Meng Y, Jiang H, Du L, Wu Q, Li S, Luo S, Li M, Xiao L, He H, He X, Yu Q, Fang J and Lu Z. Aerobic glycolysis promotes tumor immune evasion by hexokinase2-mediated phosphorylation of IκBα. Cell Metab 2022; 34: 1312-1324, e1316.
[44] Li T, Niu M, Zhou J, Wu K and Yi M. The enhanced antitumor activity of bispecific antibody targeting PD-1/PD-L1 signaling. Cell Commun Signal 2024; 22: 179.
[45] Leuzzi G, Vasciaveo A, Taglialatela A, Chen X, Firestone TM, Hickman AR, Mao W, Thakar T, Vaitsiankova A, Huang JW, Cuella-Martin R, Hayward SB, Kesner JS, Ghasemzadeh A, Nambiar TS, Ho P, Rialdi A, Hebrard M, Li Y, Gao J, Gopinath S, Adeleke OA, Venters BJ, Drake CG, Baer R, Izar B, Guccione E, Keogh MC, Guerois R, Sun L, Lu C, Califano A and Ciccia A. SMARCAL1 is a dual regulator of innate immune signaling and PD-L1 expression that promotes tumor immune evasion. Cell 2024; 187: 861-881, e832.
[46] Shi K, Chen Y, Gao T, Guo H, Fu X, Wu Y and Yu H. The oncogenic role of UBXN1 in gastric cancer is attributed to the METTL16-mediated m6A methylation and histone modifications. Cancer Med 2025; 14: e70772.
[47] Wei W, Zhang ZY, Shi B, Cai Y, Zhang HS, Sun CL, Fei YF, Zhong W, Zhang S, Wang C, He B, Jiang GM and Wang H. METTL16 promotes glycolytic metabolism reprogramming and colorectal cancer progression. J Exp Clin Cancer Res 2023; 42: 151.
[48] Li J, Yang F, Wang Z, Zheng S, Zhang S, Wang C, He B, Wang JB and Wang H. METTL16-mediated N6-methyladenosine modification of Soga1 enables proper chromosome segregation and chromosomal stability in colorectal cancer. Cell Prolif 2024; 57: e13590.

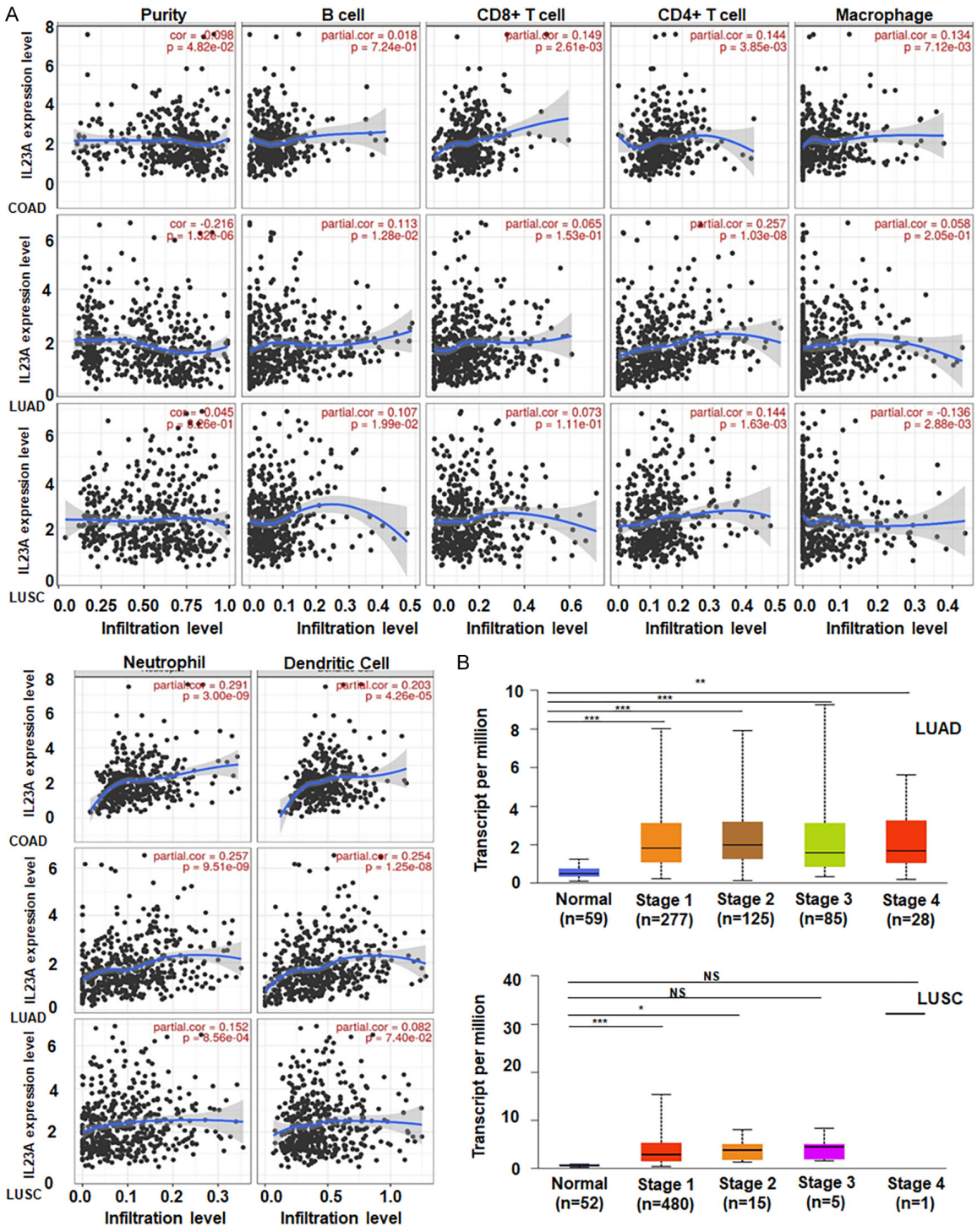

Figure S1. IL23A expression correlates with immune cell infiltration and tumor progression. A. Scatter plots showing correlations between IL23A expression and the infiltration levels of immune cells - including B cells, $CD8^+$ T cells, $CD4^+$ T cells, macrophages, neutrophils, and dendritic cells - in COAD, LUAD, and LUSC samples from the TIMER database. Each plot includes Pearson correlation coefficients and *p*-values indicating significant associations. B. Box plots illustrating IL23A expression in LUAD across clinical stages and in LUSC across histological subtypes. IL23A expression increases with advancing tumor stage in LUAD and varies significantly among LUSC subtypes. Statistical significance is indicated by *p*-values.

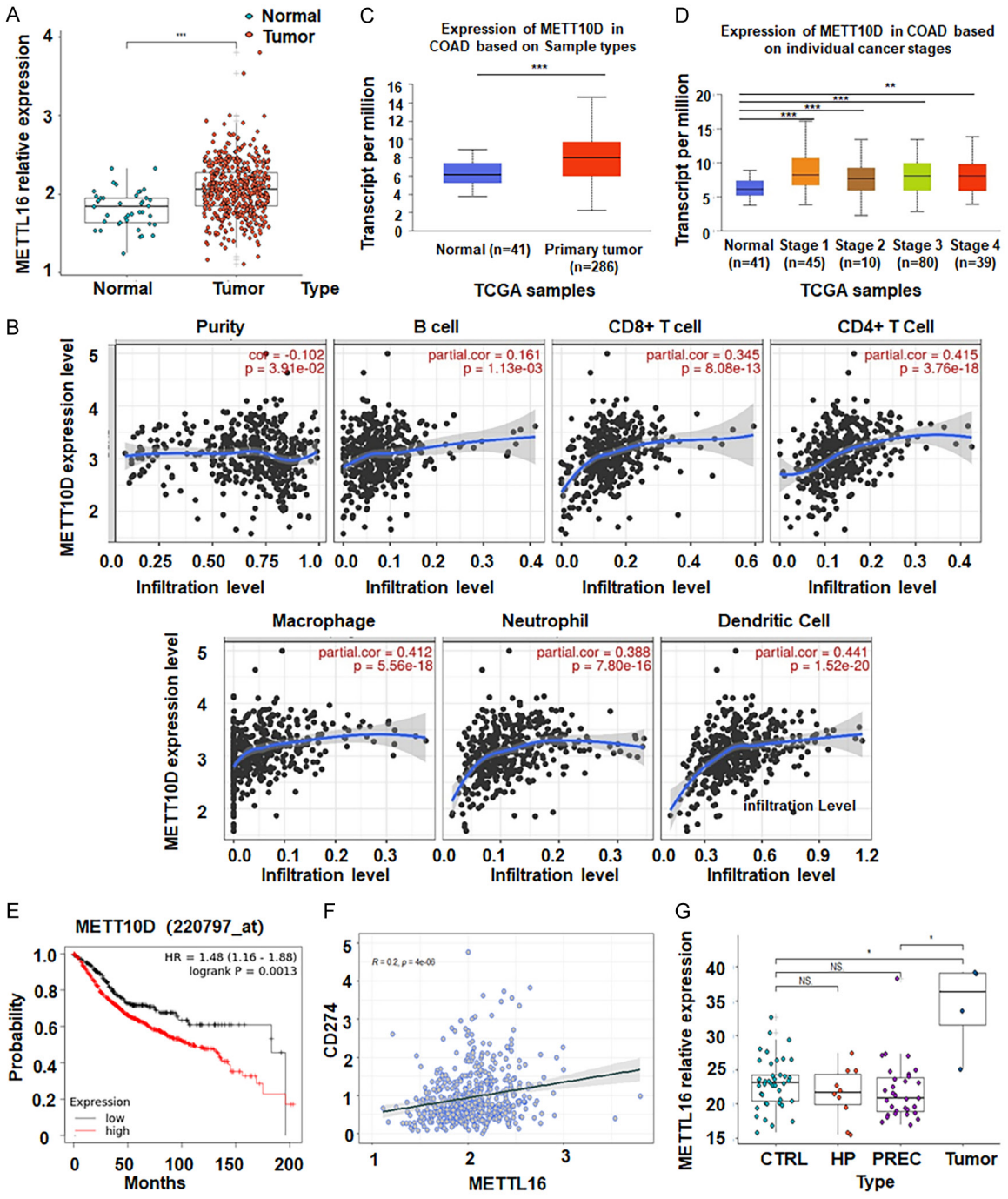

Figure S2. Expression levels and clinical significance of METTL16 in tumor tissues. A. Scatter plot comparing METTL16 expression in normal and tumor tissues across TCGA samples. Each point represents an individual sample; red denotes tumor and blue denotes normal tissue. METTL16 expression is significantly higher in tumors. B. Correlation analysis between METTL16 expression and immune cell infiltration levels in COAD. Scatter plots illustrate relationships with B cells, $CD8^+$ T cells, $CD4^+$ T cells, macrophages, neutrophils, and dendritic cells. Correlation coefficients (cor) and partial correlations (partial.cor) are provided. C. Box plot comparing METTL16 expression in normal and tumor tissues from COAD samples. Expression is significantly elevated in tumors ($P < 0.0001$). D. Box plot showing METTL16 expression across cancer stages in COAD, with a trend of increased expression in later stages. Statistical significance is denoted by *p*-values. E. Kaplan-Meier survival curve for COAD patients stratified by METTL16 expression. High METTL16 levels correlate with poorer overall survival. Log-rank *p*-value and hazard ratio (HR) are indicated. F. Scatter plot showing a significant positive correlation between METTL16 and IL23A expression in COAD (R = 0.20, $P = 4.2e\text{-}06$). G. Box plot comparing METTL16 expression across sample types (normal, hyperplastic, precancerous, tumor). METTL16 levels are significantly elevated in tumor tissues ($P < 0.0001$).

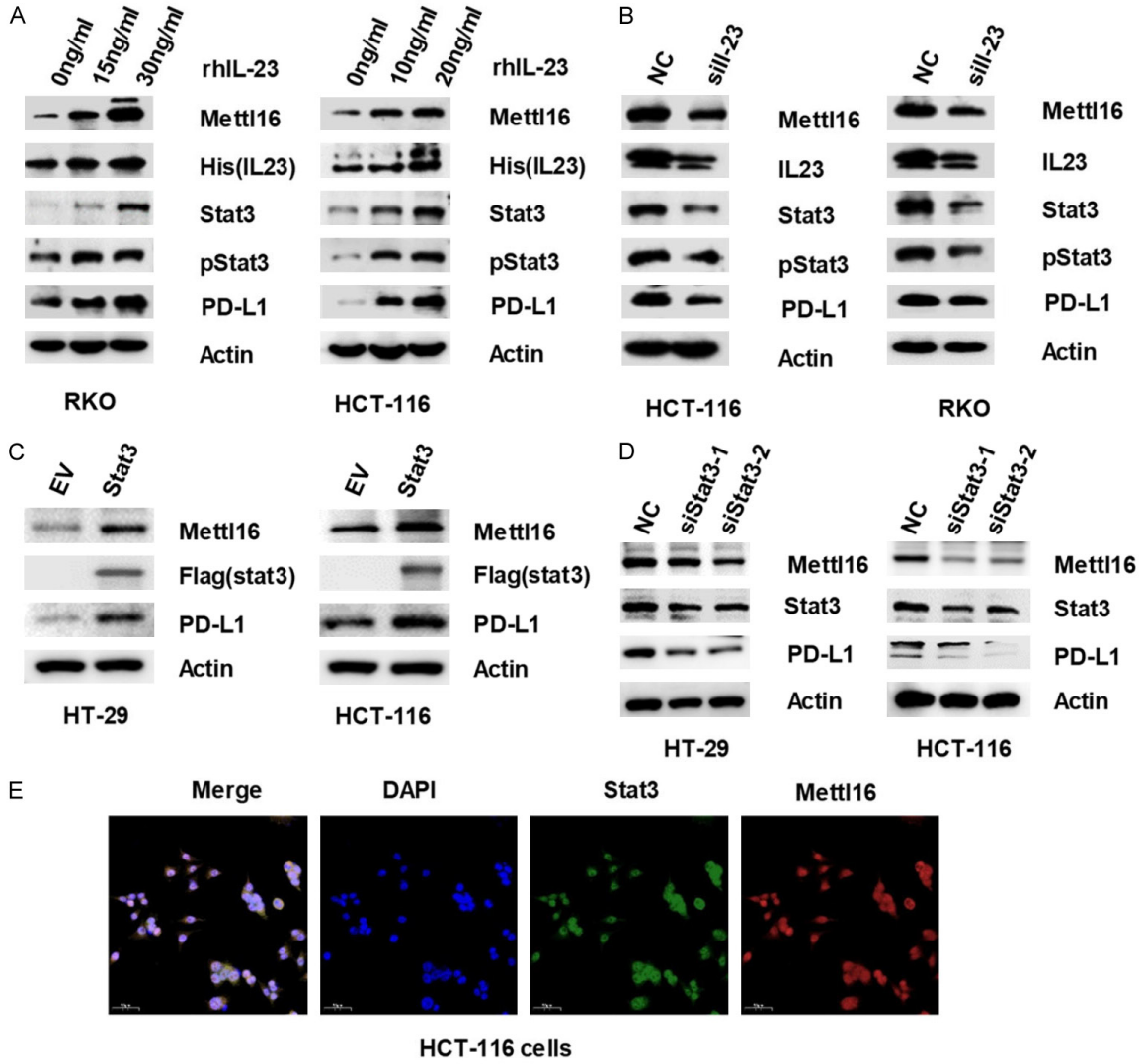

Figure S3. IL-23 induces METTL16 expression and modulates PD-L1 in various cancer cell lines. A. Western blot analysis of METTL16, His-tagged IL-23, STAT3, phospho-STAT3, PD-L1, and Actin in RKO and HCT-116 cells treated with 0, 10, or 20 ng/mL rhIL-23 for 24 hours. B. Western blot analysis of METTL16, endogenous IL-23, STAT3, p-STAT3, PD-L1, and Actin in HCT-116 and RKO cells transfected with siIL-23 or NC. C. Western blot showing METTL16, PD-L1, Flag-STAT3, and Actin levels in HT-29 and HCT-116 cells transfected with EV or Flag-STAT3. D. Western blot of METTL16, STAT3, PD-L1, and Actin in HT-29 and HCT-116 cells transfected with NC, siMETTL16, siSTAT3-1, or siSTAT3-2. E. Immunofluorescence analysis of HCT-116 cells showing nuclear co-localization of METTL16 and STAT3. DAPI stains nuclei (blue), and merged images indicate overlap.

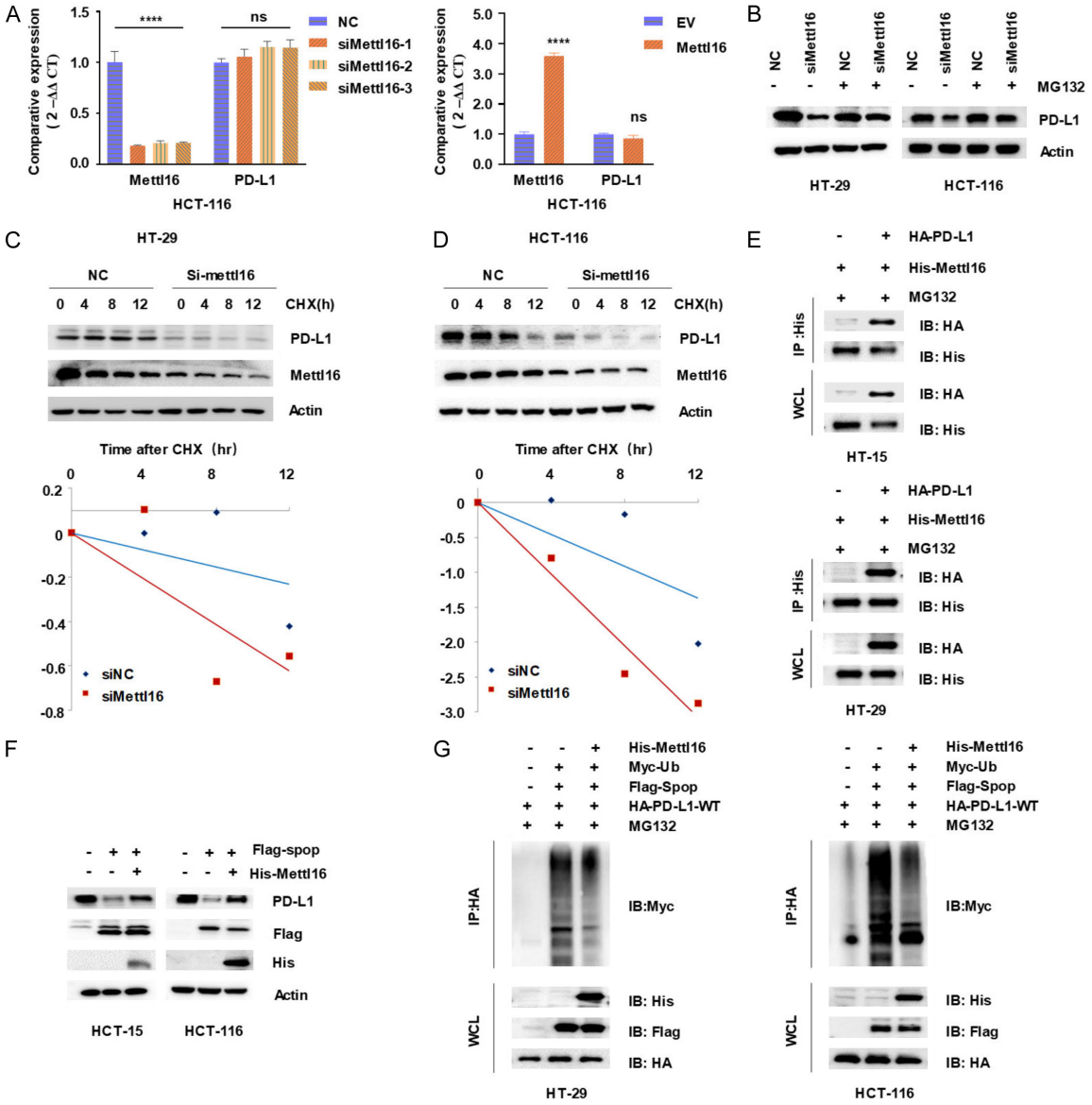

Figure S4. METTL16 inhibits SPOP-mediated PD-L1 ubiquitination and degradation. (A) qRT-PCR analysis of METTL16 and PD-L1 mRNA levels in HCT-116 cells transfected with METTL16 siRNA or empty vector (EV). Left: METTL16 knockdown group; Right: METTL16 overexpression group. (B) Western blot analysis of PD-L1 expression in HT-29 and HCT-116 cells transfected with METTL16 siRNA or NC, with or without treatment with the proteasome inhibitor MG132 (10 μM for 6 h). (C, D) Western blot of PD-L1 and METTL16 in HT-29 (C) and HCT-116 (D) cells transfected with METTL16 siRNA or NC. Cells were treated with cycloheximide (CHX, 20 μg/mL) for 0, 4, 8, or 12 hours to assess PD-L1 stability. (E) Immunoblot (IB) analysis of immunoprecipitates (IPs) and whole-cell lysates (WCLs) from HT-15 cells transfected with the indicated plasmids. MG132 (10 μM) was applied 6 h before harvesting. (F) IB analysis of WCLs from HT-29 and HCT-116 cells transfected with the indicated plasmids to assess PD-L1 and SPOP expression. (G) Ubiquitination assay via IB of IPs and WCLs from HT-29 and HCT-116 cells transfected with the indicated constructs. MG132 treatment (10 μM for 6 h) was applied prior to sample collection.

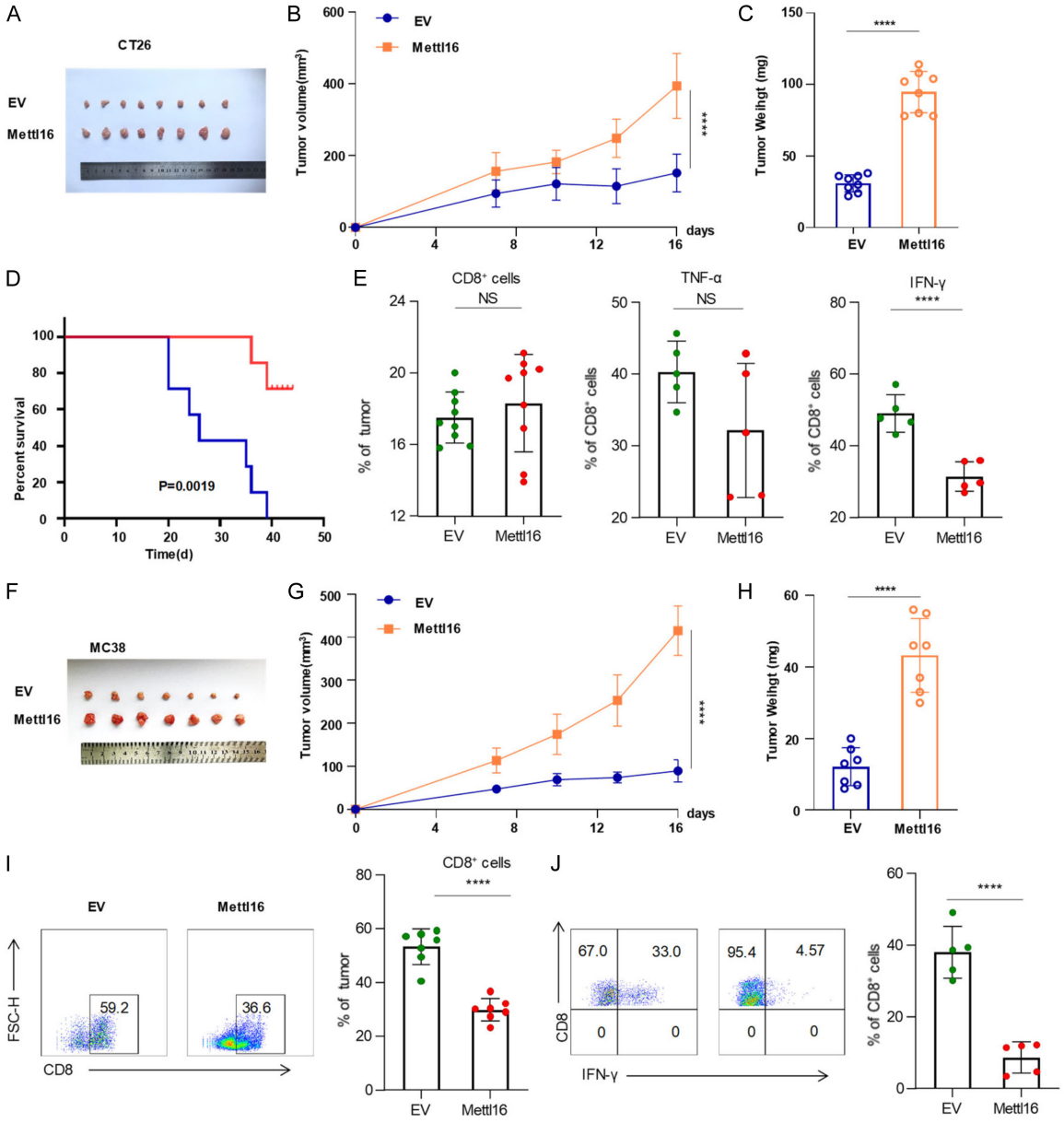

Figure S5. METTL16 promotes tumor growth and immune evasion in vivo. A. CT26 cells overexpressing METTL16 or EV were injected into BALB/cmice. Tumor volume was measured over 16 days. METTL16 significantly promoted tumor growth ($P < 0.0001$). B. Tumor weights at endpoint confirmed increased tumor burden in the METTL16 group ($P < 0.0001$). C. Representative images of tumors from EV and METTL16-overexpressing groups. D. Flow cytometry of tumor-infiltrating CD8⁺ T cells showing reduced abundance in METTL16-overexpressing tumors. E. IFN-γ secretion by CD8⁺ T cells was significantly lower in METTL16-overexpressing tumors compared to control ($P < 0.0001$). F. MC38 cells transfected with EV or METTL16 overexpression plasmid were subcutaneously injected into C57BL/6 mice. Tumor volume was monitored over 16 days. METTL16 significantly enhanced tumor growth ($P < 0.0001$). G. Tumor weight data corroborated the increased growth in the METTL16 group ($P < 0.0001$). H. Representative tumor images from EV and METTL16 groups. I. Kaplan-Meier survival analysis revealed significantly shorter survival in mice bearing METTL16-overexpressing tumors ($P = 0.0019$). J. Flow cytometry analysis showed reduced infiltration of CD8⁺ T cells and suppressed cytokine secretion (TNF-α, IFN-γ) in METTL16-overexpressing tumors ($P < 0.0001$ for IFN-γ).

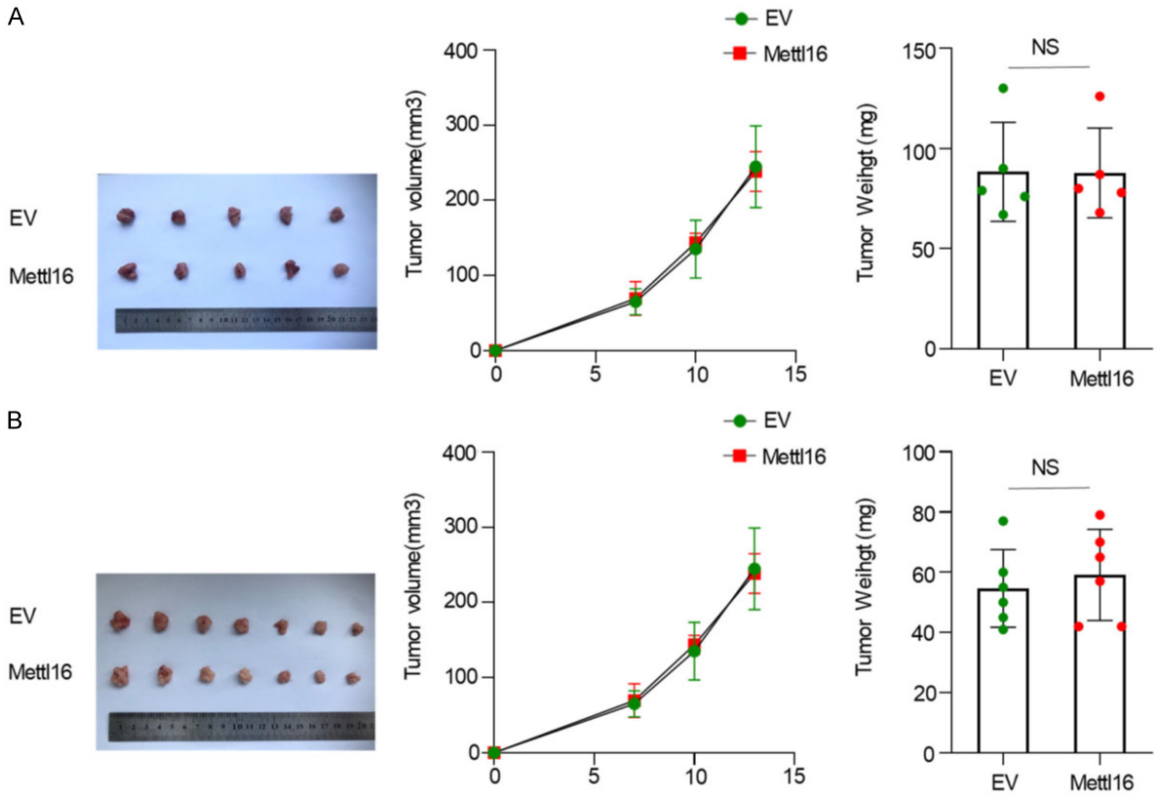

Figure S6. METTL16 fails to promote tumor growth in immunodeficient nude mice. A. CT26 cells transfected with EV or METTL16 were injected into BALB/c mice. Tumor volumes were measured over 15 days. METTL16 overexpression significantly increased tumor growth. Representative tumor images are shown. No significant difference in final tumor weight was observed. B. MC38 cells overexpressing METTL16 or EV were injected into C57BL/6 mice. Tumor volumes were recorded over 15 days. METTL16 significantly promoted tumor growth, although no significant difference in tumor weights was observed. Representative tumor images are shown.